N71-25611

A CONCEPTUAL STUDY OF A MOMENTUM WHEEL STABALIZED GEOSTATIONARY AERONAUTICAL SATELLITE

W. N. Redisch, et al

Goddard Space Flight Center
Greenbelt, Maryland

January 1971

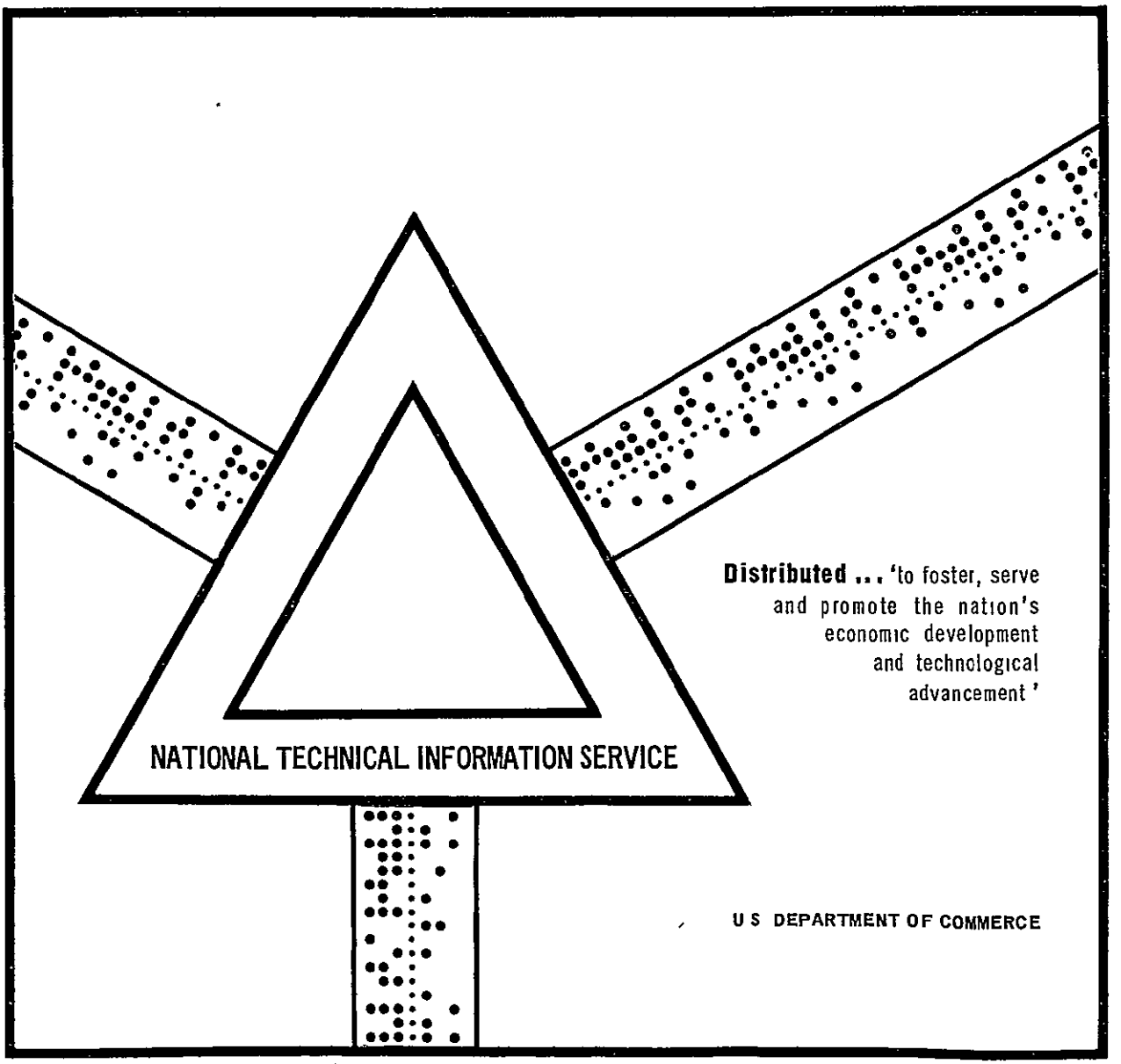

X-490-71-78
PREPRINT

NASA TM X- 65509

A CONCEPTUAL STUDY OF A MOMENTUM WHEEL STABALIZED GEOSTATIONARY AERONAUTICAL SATELLITE

W. N. REDISCH
A. F. WHITE
G. GOLDBERG

JANUARY 1971

GSFC — GODDARD SPACE FLIGHT CENTER —
GREENBELT, MARYLAND

A CONCEPTUAL STUDY

OF A

MOMENTUM WHEEL STABILIZED

GEOSTATIONARY AERONAUTICAL SATELLITE

Dr. W. N. Redisch

A. F White

G. Goldberg

January 1971

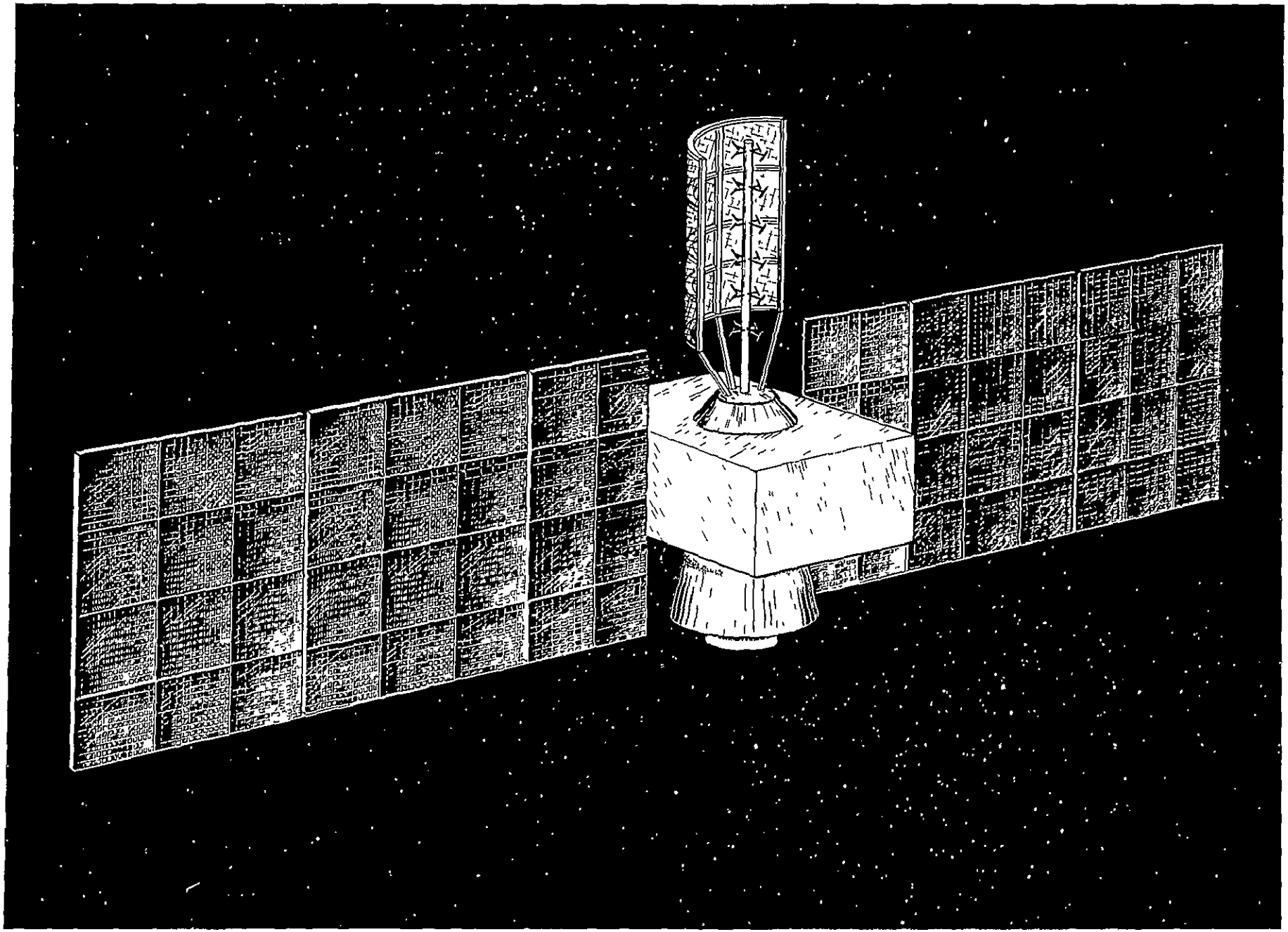

TABLE OF CONTENTS

LIST OF ILLUSTRATIONS

LIST OF ILLUSTRATIONS (Continued)

LIST OF ILLUSTRATIONS (cont'd)

FOREWARD

During 1970 GSFC personnel were actively engaged in studies in support of the definition of an aeronautical satellite system for the oceanic region. The conceptual spacecraft design in this report was performed by the Space & Electronics System Division, Fairchild-Hiller Corporation, Germantown, Maryland, on contract NAS5-11822 in support of the studies and under the direction of the authors.

The material presented in this report is the preliminary result of a conceptual design study and, therefore, should not be considered final. As such, some hypotheses presented are not proven and require further investigation. In particular, the center of pressure-center of gravity offset, which is thought to be 0.5 inches, requires further verification. The L-Band antenna design including the possible use of an R-F rotary joint also requires further investigation. It should also be noted that lesser antennas such as the C-Band and whip antennas are not shown, but other deployment schemes can be used which would enable an increase in transfer orbit power, if required. The report demonstrates that a 1200 watt (start of life, unregulated power) satellite with a 15% weight growth margin is feasible in accordance with the mission guidelines contained herein. It also describes a reliable attitude and orbit control concept which does, however, require further analysis.

1.0 INTRODUCTION

This volume presents the conceptual design and analysis of a synchronous equatorial satellite utilized for a NASA/ESSRO experimental/pre-operational aeronautical satellite system (NETCOS)*. The concept studied herein is a momentum wheel stabilized, sun-oriented satellite, with a North Atlantic pointing antenna. The 1200 watt satellite is launched on the Delta launch vehicle and utilizes an apogee engine to achieve synchronous equatorial orbit.

The study guidelines are tabulated in Section 2.0, as well as the mission sequence of operation. Design compatibility with most of the guidelines stated has been verified and the corresponding data is included in this report. However, verification of some of the guidelines require more detailed analysis than that normally performed during a conceptual study effort.

Sections 3.0 through 5.0 contain a complete design description of the spacecraft including a layout drawing and mass properties tabulations. It should be noted that the material included is primarily of a mechanical nature (with the exception of the antenna analysis) since the communications, power, telemetry, and command systems were considered fixed at the outset of this study.

Section 6.0 describes the attitude and orbit control requirements and design. This section includes operation descriptions as well as descriptions of the hardware utilized.

* The achronym "NETCOS" was established at the onset of the study and does not refer to an accepted program achronym.

2.0 GUIDELINES AND MISSION SEQUENCE

2.1 GUIDELINES

2.1.1 Orbit

(a) Synchronous equatorial

(b) Two (+ one) spacecraft in orbit

(c) Maximum shadow = 72 minutes

2.1.2 Launch Vehicle - Delta 904

(a) Delta + 9 castor + TE-M-364-4

(b) Fairing - 7-foot fairing

(c) One spacecraft per launch

(d) Vehicle will inject spacecraft into a 100 X 19,323 N.M. orbit.

(e) Standard adapter - 45#.

2.1.3 Technology

(a) Use available technology, space qualified when possible

(b) Five year desirable life time, 3 year minimum

2.1.4 Spacecraft

The spacecraft shall be sun oriented and momentum wheel stabilized. The spacecraft design shall be capable of longterm (approx. 1 month) spin survival in the transfer trajectory mode with a spin axis orientation that is favorable for solar power generation. During this mode, no surveillance must be performed and the main antenna will not be operative or despun.

2.1.4.1 Stabilization - The spacecraft shall be spin stabilized during the transfer orbit and momentum wheel stabilized in synchronous orbit. The spacecraft shall be capable of spin stabilization in synchronous orbit as a failure mode of operation.

2.1.4.2 Power

(a) 1200 watt, start of life raw power solar array.

(b) Assume solar cells and rechargeable batteries

(c) Design solar array and battery for the following loads:

1. 150 watts operational capability in shadow (90 for housekeeping, 60 for surveillance).
2. 50 watts operational capability during the transfer orbit.

2.1.4.3 Communications

(a) Assume a combination of L and C bands

(b) Assume parabolic reflector with at least 22 db gain on the axis and a 9.5^{o} by 12.2^{o} half power beam width

(c) Provide VHF capability for spacecraft telemetry and command during launch and transfer orbit

2.1.4.4 Structure - Lightweight design utilizing standard spacecraft construction.

2.1.4.5 Propulsion and Controls

(a) Assume a solid propellant motor on the spacecraft for circularizing the transfer orbit and removing its inclination.

(b) Assume hydrazine liquid propulsion subsystem for injection error correction, orbital trim, attitude control, and

eventual spin control (if required). Velocity impulse for orbit control shall be 360 f.p.s.

(c) No N-S station keeping

(d) 1/2 degree accuracy about all three axes.

2.1.4.6 Thermal

(a) Maintain hydrazine at 5°C or above

(b) Maintain battery between o°C and 10°C.

2.1.4.7 Attitude Determiniation

(a) Earth sensor required

(b) Sun sensor(s) required.

2.1.4.8 Weight

(a)* Maximum injection weight = 1255# (excluding adapter)

(b) Provide weight contingency = 15% of the maximum possible spacecraft weight <u>after</u> apogee motor firing.

2.1.4.9 Inertia

The spacecraft configuration shall have a favorable ratio of inertias for spin stability in both the stowed and deployed configuration.

2.2 MISSION SEQUENCE

(a) Liftoff

(b) Third stage spin-up to 80 RPM, nominal

(c) Third state ignition

(d) Third stage burnout

(e) Spacecraft injection into 100 X 19,323 N.M. 28.5 - degree inclined transfer orbit at the equator

* Updated maximum injection weight is shown in Appendix B.

(f) Spacecraft Separation and partial despin to 45 RPM. (Spacecraft spin axis in plane of transfer orbit.)

(g) Ground tracking of spacecraft to determine transfer orbit injection errors.

(h) Reorientation of spacecraft spin axis to proper attitude for apogee motor firing.

(i) Verification that spacecraft attitude is correct for apogee motor firing. Ground station will verify attitude by POLANG/TM data from the spacecraft attitude sensors.

(j) Apogee motor firing (approximately 36 seconds firing).

(k) Ground tracking of spacecraft to determine spacecraft orbit.

(l) Initial Correction of in plane orbit errors using hydrazine system.

(m) Despin spacecraft.

(n) Deploy solar array panels.

(o) Acquire reference sun oriented attitude.

(p) Final correction of synchronous-orbit errors.

(q) Uncage the reflector or reflector drive motor.

(r) Start reflector drive motor.

(s) Turn on navigation communications and begin operation.

9. Locate the solar array and antenna such that the center of pressure of the spacecraft is coexistent with the spacecraft C.G. (This establishes the upper frustrum.)

10. Arrange the black boxes within the module to establish the actual spacecraft C.G. with designated C.G. Note: Propellant tanks C.G. should be inplane with spacecraft C.G.

3.3 DESIGN DESCRIPTION

The spacecraft configuration of Figure 3.1 includes a thermally controlled rectangular module containing the attitude control telemetry and other subsystems. Attached to the sides of the spacecraft module are two (2) 600 square foot solar arrays (1200 watt start of life power) subdivided into three folding panels. The design represents approximately a 14 watt pound start of life solar array. Mounted forward on the spacecraft is a parabolic cylinder antenna using a fixed omnidirectional feed. Packaged within the spacecraft body is a TE-M 442 apogee motor. The spacecraft assembly is supported to the Delta adaptor with a frustrum thrust cone. Note the use of the standard TE-M 442 enables the spacecraft C.G. to be lowered six inches.

The module frame is constructed of aluminum extrusions. Attached to the framework are four honeycomb side panels. These panels support the equipment within the spacecraft. The high thermal dissipators are located on the dark side. The relatively temperature insensitive units are mounted on the sun side. Thermal heat pipes are located within the sandwich panels to assist in temperature control. The rectangular section of the structure is attached to a central sheet metal thrust cylinder 29 inches in diameter by honeycomb sandwich bulkheads and external stabilizing struts. The apogee motor is located within this cylinder. Four attitude control gas propellant tanks are attached to the outer

3.0 SPACECRAFT DESIGN

3.1 GENERAL

A design approach was determined which would best enable the spacecraft to meet the guidelines presented in Section 2.0. Utilizing the established design approach led to the spacecraft design which is described in this section.

3.2 DESIGN APPROACH

1. Designate the Delta separation plane as the primary reference.
2. Establish the dynamic envelope.
3. Locate the apogee engine relative to the separation plane.
4. Determine the C.G. of PROPELLANT (center of burn) of the apogee engine.
5. Designate C.G. of the spacecraft at the center of burn.
6. Define the solar array based on the power requirement consistent with the spacecraft module profile.
7. Design and locate the spacecraft module such that the spacecraft module C.G. is coexistent with the spacecraft C.G. (This will establish the lower frustrum.)
8. Locate the spacecraft antenna relative to the solar array for proper clearance.

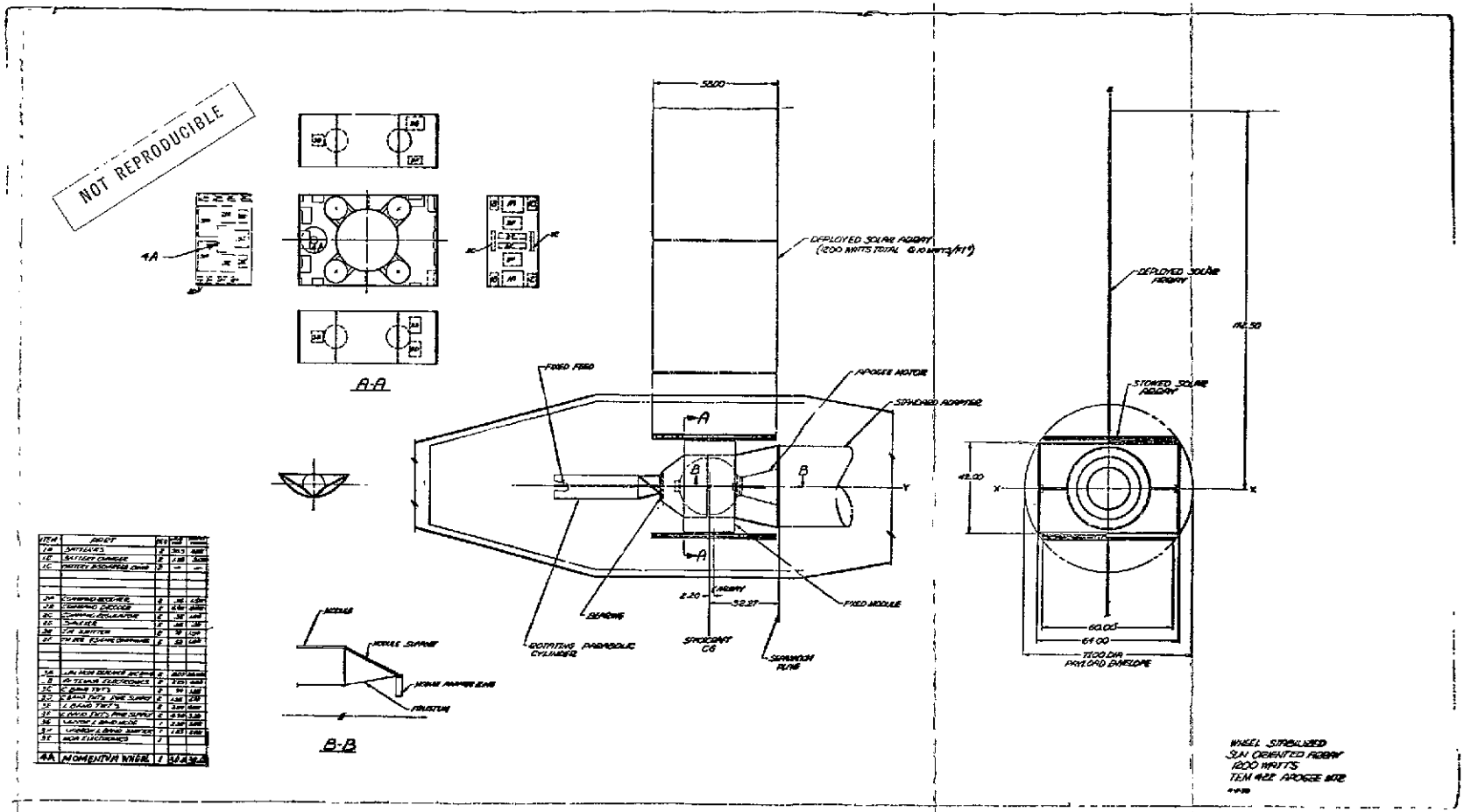

FOLDOUT FRAME 1

FOLDOUT FRAME 2

Fig. 3.1 Re

surface of the thrust cylinder. These tanks are strap-mounted and the mounts contain expansion capability to allow for tank expansion. Four access covers are located on the top and the bottom of the module to provide convenient access to the interior of the spacecraft.

A sheet metal frustum added forward of the central thrust cylinder supports the antenna assembly. A platform mounted on the forward end of the frustum contains a bearing and drive unit. Trusses support the honeycomb reflector. The non-rotating feed is fixed to the spacecraft and is omnidirectional. Access doors are provided for quick and convenient access.

The solar array is deployed from the spacecraft module. Two outboard panels 58" x 60", and one inboard panel 58" x 30, are used on each side of the spacecraft. The panels are honeycomb sandwich low gage aluminum facings. The array will produce 1200 watts of electrical power.

The spacecraft is supported during launch by a honeycomb thrust frustum. The frustum is attached to the adaptor using a marman-type clamp.

4.0 · COMMUNICATION SUBSYSTEM

The system provides voice and data channels on each satellite. The nominal goal for word intelligibility should be 95% for at least 95% of a message (articulation index of about 0.6). The data channel capacity is to be 1200 bits per second with a maximum bit error rate of 10^{-5}.

Both analog and digital methods of voice processing and modulation may be considered for the voice channels. Amplitude and frequency truncation along with narrow-band FM may be considered as an analog candidate. PCM, delta modulation (and its variations) and pulse duration modulation, all coupled with DPSK, may be the digital candidates. One of the major difficulties underlying the selection is the lack of a good quantitative method of comparing the channel performance of the various techniques.

The communication subsystem receives signals at C-band and L-band (see Figure 4.1). The signals are amplified, filtered, and converted to the intermediate frequency. The signals are then directed to one of three IF amplifiers, where they are further amplified and filtered. The output signals of the IF amplifiers are directed to the transmitter, up-converted, filtered, and amplified to the power level required for transmission, in either C-band or L-band.

The transponder has flexibility, in that signals received in any band may be switched to any of the frequency bands for transmission.

The transponder makes efficient use of three identical IF amplifiers, in that any one of the IF amplifiers may be switched (by ground

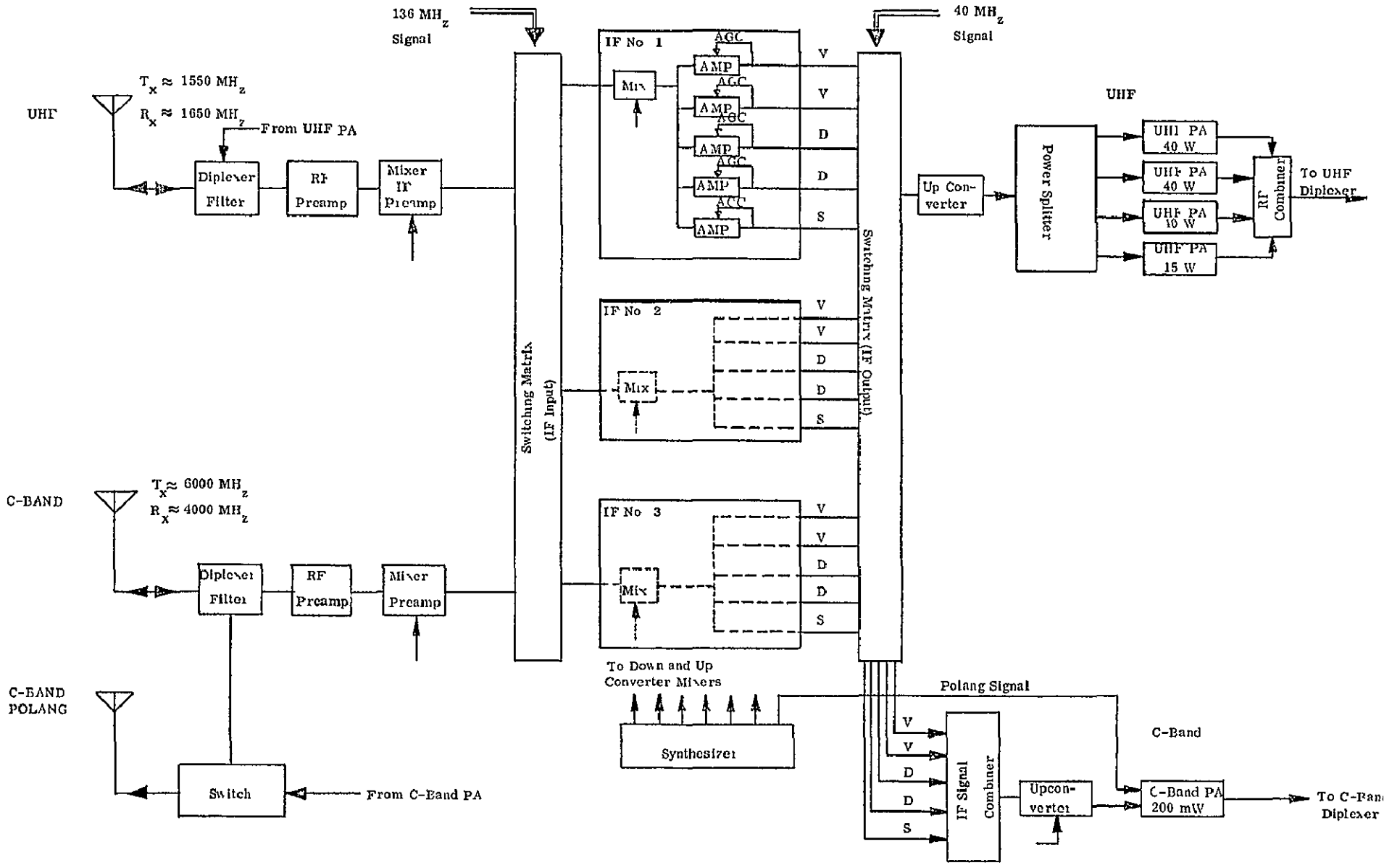

Figure 4.1 Integrated Communications Transponder (L-Band)

command) to any one of the received signals. Redundancy at IF is achieved economically, by means of switching.

The transponder has good reliability, in that up-and-down-converters, IF amplifiers, local oscillators, and power amplifiers are redundant.

The communication subsystem utilizes an L-band reflector-type antenna with unequal beamwidths which provide near optimum coverage. A small electromagnetic horn provides the coverage needed for the C-band communication links to the satellite control centers. During the transfer orbit, a low-level signal, with small cross-polarized component, will be radiated from a C-band dipole array, and will provide the signal needed for polarization angle measurements.

For purposes of this study the coverage areas reflected in the system guidelines have been used. Further studies of the operational situation may result in slightly different coverage requirements. Small changes in the reflector antenna (at L-band) and in the horn antenna (at C-band) may accommodate the new requirements.

The communication subsystem avoids the need for new and unproven components and techniques. Lengthy and expensive development efforts are thus obviated. The exception may lie in the area of L-band, solid-state, power amplifiers, where values of efficiency, reliability, and cost are not as well defined as at lower frequencies.

With the present spacecraft design, the weight margin is 14.5%, this margin is sensitive to aircraft antenna gain, as can be seen from the Figure 4.2, and to the number of channels. In the figure, a UHF channel

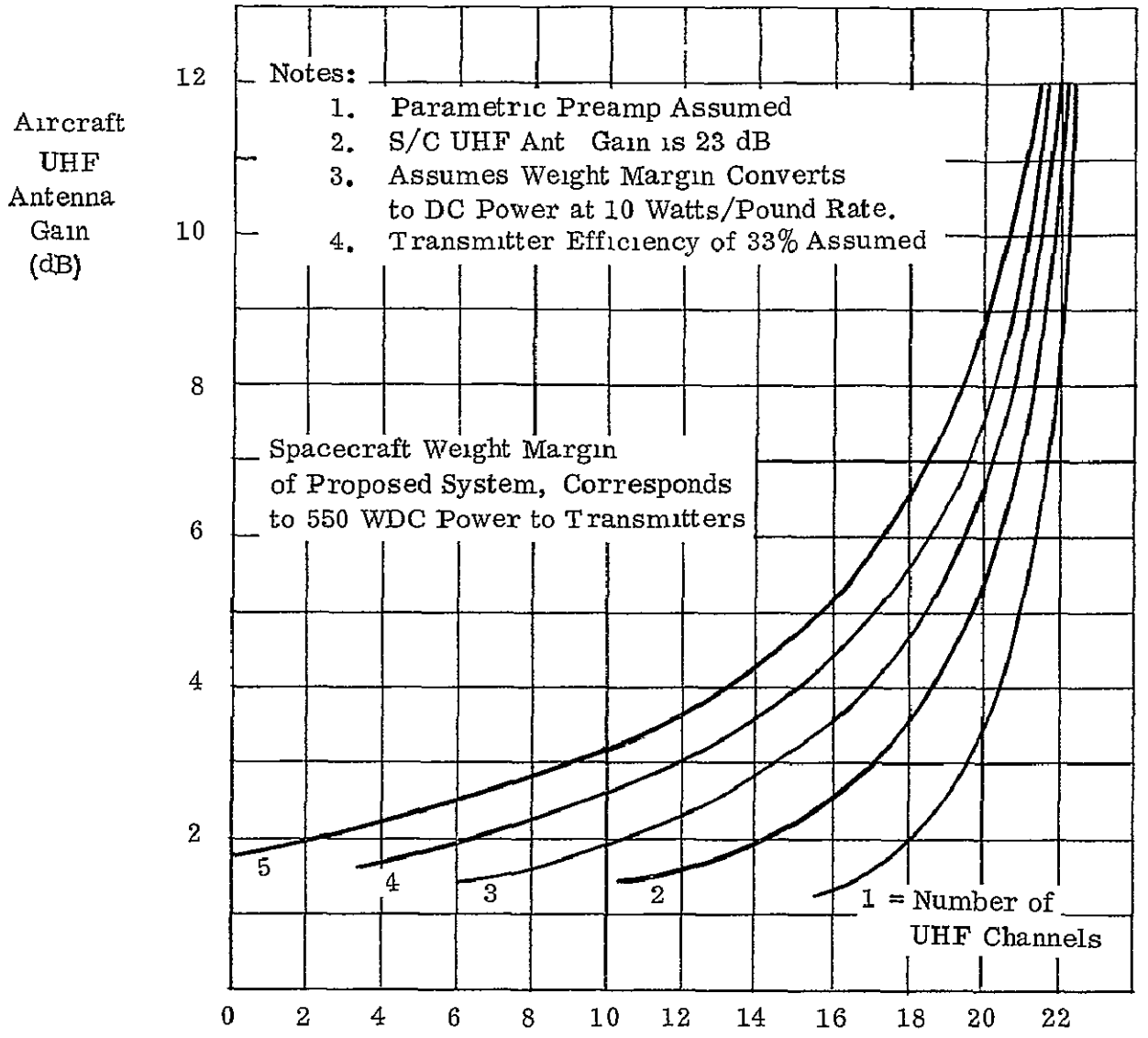

Fig. 4.2 Aircraft UHF Antenna Requirements Vesus Spacecraft Weight Margin

consists of one voice channel, one digital channel, and one surveillance channel. For the present design, L-band antenna gains (on the aircraft) must be at least 1 db (for a single channel) and at least 4 db, for four channels. The spacecraft baseline design provides 571 watts of power for the communication transponder, at end of life. Of this amount, 550 watts are allocated to the transmitters. Initial capacity of the solar array is 1200 watts. These power requirements were determined as follows:

The general equation for energy balance is:

$$P_A t_D = P_{LD} t_D + \frac{P_{LN}}{DR} \frac{1}{B} t_N$$

where:

P_A = Average array power (watts),

P_{LD} = Average regulated day load power (watts)

P_{LN} = Average regulated nightime load power (watts) = 130 watts

t_D = Satellite day = 22.83 hours

t_N = Satellite night = 1.16 hours

B = Battery discharge to charge efficiency = 0.56

DR = Battery discharge regulator efficiency = 0.85

Using the indicated values, it is found that the array power and the regulated day load power are related by the following:

$$P_A = P_{LD} + 13.9 \quad (1)$$

To insure sufficient array power at the end of life (EOL), all factors which cause a decrease in power must be taken into account in the determination of the beginning of life (BOL) requirement.

The factors which cause a decrease in power are the following:

K_1 = percentage power remaining after charged particle irridiation damage (assume 75% for five years)

M = design margin, this includes the power loss associated with ultraviolet light damage, array blocking diode voltage and line drop, changes in solar intensity, etc. (assume 90%)

= angle between spacecraft orbit plane and incident solar radiation (assume solstice sun angle of 23.5° worst case plus 2.5° attitude inclination angle).

The average array power, at end of life and for the worst sun angle, is

$$P_{A\ (EOL)} = K.M \cos P_{A\ (BOL)}$$

$$= 0.75 \times 0.90 \times 0.899 \times P_{A\ (BOL)}$$

$$= 0.606\ P_{A\ (BOL)} \qquad (2)$$

From equations (1) and (2) the regulated day load power, at the end of the mission and for the worst sun angle, is

$$P_{LD\ (EOL)} = \frac{P_{A\ (BOL)} - 23}{1.65}$$

For the assumed 1200 watt solar array (with 60 watts reserved for contingencies),

$$P_{A\ (BOL)} = 1200 - 60 = 1140 \text{ watts}$$

and hence

$$P_{LD\ (EOL)} = \frac{1140 - 23}{1.65} = 676 \text{ watts}$$

The available load power is allocated as follows:

Telemetry and Command	18 watts
Attitude Control	42
Communications	571
Power	45
	676 watts

At the beginning of the mission, the array has not suffered particle radiation damage and the regulated day load power is 907 watts, which is allocated as follows:

Telemetry and Command	18 watts
Attitude Control	42
Communications	802
Power	45
	907 watts

At the present stage of conceptual spacecraft design, it is desirable to have a spacecraft weight margin of 15%. To provide the desired two channels requires an aircraft antenna gain of 2 db. This value is reasonable and practical and, consequently, the confidence level in the spacecraft design is high.

4.1 PRELIMINARY ANTENNA DESIGN AND ANALYSIS

Since the main spacecraft module is sun oriented and the L-Band antenna must be earth oriented, the antenna must rotate at a rate of one revolution per orbit relative to the main spacecraft module. Due to the apparent lack of a qualified L-Band R-F rotary joint and the possible reliability problems associated with such a device it was deemed advisable to investigate a fixed feed antenna design.

A parabolic cylinder rotating about a fixed line feed is the most advantageous when considering weight, moments of inertia, and solar pressure torques. However, several feed design problems are associated with this approach and these are discussed in this section of the report.

4.2 GAIN CALCULATION

Since a 12.2° x 9.5° Beam is required - The "a" and "b" dimensions of the cylinder must be as follows:

a = 31.5 inch, to produce HPBW of 12.2° [1/]

b = 37.2 inch, to produce HPBW of 9.5°

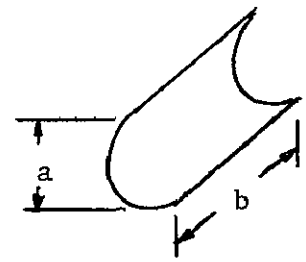

The Gain of this antenna based on a f/d ratio of 0.18 (ψ = 216°) is as follows:

Aperture eff.	97%
Spillover eff.	60%
Miscellaneous [2/]	90%
	52.4%

$$\text{Gain} = 52.4 \text{ percent of } \frac{4\pi A}{2} = 22.0 \text{ dB}$$

A Parabolic dish in comparison would have a 23.4 dB gain minus a.2 dB loss due to the rotary joint or a 23.2 dB gain. (Based on a 60% efficiency)

"a" dimension would be 40 inches to produce HPBW of 12.2° and

"b" dimension would be 50 inches to produce HPBW of 9.5°

For a parabolic cylinder with a f/d = 9.18, the angle subtended by reflector at the focal line 216 degrees. The power radiated by the feed and intercepted by the reflector is, thus,

---

1/ Approximate. This beamwidth is controlled by feed array characteristics, which will be discussed later.

2/ Includes polarization, blockage (1 inch diameter cylinder), surface inacurracy, and phase effects.

216/360 = 0.60 = 50%. (spillover efficiency)

If linear polarization were used, the focal length f could be adjusted so that back lobe radiation from feed is in phase with reflected radiation. This would increase the gain by the ratio:

$$1 + 2 \quad \theta_1 / \theta_2 \quad \text{approximately,}$$

where θ is the HPBW in the plane normal to the antenna axis ($\theta_1 = 12.2°$) and θ_2 is the width of the feed beam in the same plane ($\theta_2 = 360°$). For these values, $1 + 2\ \theta_1/\theta_2 = 1.3$ and the gain is increased by 1.1 dB. Optimum values of f are /4, 3 /4, 5 /4, . . . However, if the feed radiated RHPC, upon reflection, the wave is converted to LHCP. If the receiving system is designed to handle LHPC, it will respond to the orthogonal polarization and no improvement can be realized by barying f.

The block efficiency is estimated for blockage by a one inch diameter feed line.

4.3 ARRAY CONSIDERATIONS

Requirements are that they array be (1) omnidirectional (so that it will illuminate the reflector properly, irrespective of the reflector angular location), (2) circularly polarized, and (3) produced a 95° beam in the plane parallel to its axis.

To reduce the number of elements and the associated complex feeding problems, it is desirable to have large spacing between elements. The position of grating lobes, as a function of spacing, is

$$\sin \theta g = \pm \frac{\lambda}{D}$$

where θg is the angular location of the unwanted grating lobe, D is the spacing between elements of the feed, and λ is the wavelength. For λ spacing

$$\sin \theta = \pm 1$$

and grating lobes are located at $\pm 90°$ (along the axis of the array). For the four-dipole element (to be described later) there is no radiation axially, and consequently, the amplitude of the grating lobe is zero.

For spacings of $3\lambda/2$, the angular location of the grating lobes is 48° (off the axis) and it is likely that significant amplitudes would also be present. For this reason, spacings in excess of λ (7 inches) have not been considered.

The requirement of circular polarization can be fulfilled by several radiating elements. The combination of a slotted cylinder (for traverse polarization) a dipole (for longitudinal polarization) could be utilized. A second alternative is a helix operating in the normal mode. A third arrangement - and the recommended one - consists of four dipoles, orientated at 45° to the feed axis, and symmetrically disposed about the feed axis. The configuration is shown in Figure 4.3. The four-dipole bay has been selected primarily because of the related work, done at 120 MHZ by Brown and Woodward (RCA Review, June 1947, pp. 259-269).

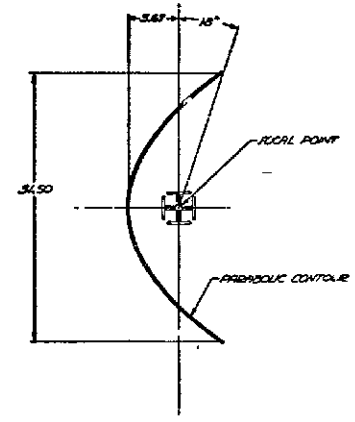

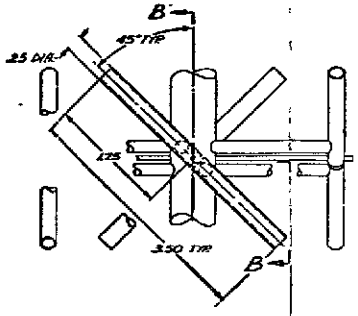

VIEW A-A
TYP 4 PLACES

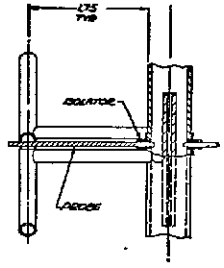

B-B

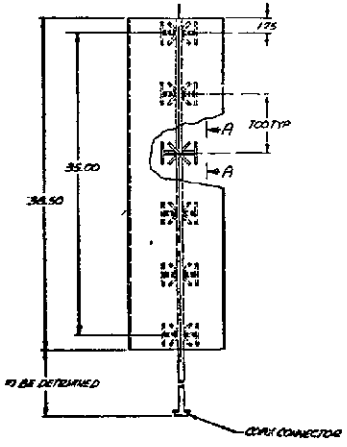

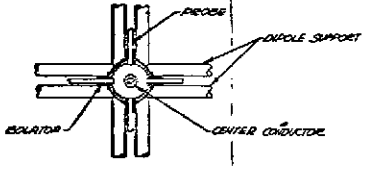

PARABOLIC CYLINDER FEED SYSTEM

D= 34.5
f= 14"
-8=0.18

Figure 4-3

FOLDOUT FRAME 1

FOLDOUT FRAME 2

To achieve good circular polarization, the four dipoles should be close together. In the present arrangement, the diameter of the circle upon which the dipoles are located is about $\lambda/2$. This diameter is felt to be somewhat large, and, if impedance considerations permit, it will be reduced. The influence of the metallic feed line up the middle of the bays is unknown. Its effect will have to be determined by experiment.

The beamwidth in the plane containing the feed should be 9.5°. Previous work showed that the aperture dimension should be 37.2 inches. This requires six bays, each consisting four dipoles, with a total length 38.5 inches (see Figure 4.3). One of the items of work to be done in the future is the calculation of the pattern, using the formulas of array theory. The result of this calculation is expected to confirm that the beam is, or very close to, 9.5° wide.

The feed arrangement recommended is a coaxial line with four dipole bays located at (almost) λ-spacing. The bay will present pure shunt loading to the line,and, consequently, the following characteristics prevail:

- There is no attenuation along the line.
- The wavelength in the line is unchanged.
- The array is uniformly illuminated, if a short-circuit is placed $\lambda/4$ beyond the last bay. The load presented to the transmitter consists of 24 dipoles, all in parallel.
- No reversal of element is required since all dipoles are in-plane.

A half-wave dipole, oriented at 45° to the vertical, and fed by a 3-wire line, is the preferred configuration for the radiating element.

Excitation will be by a capacitive probe, which extends into the main coaxial feed line (see Figure 4.1). The equivalent circuit for the element is shown below:

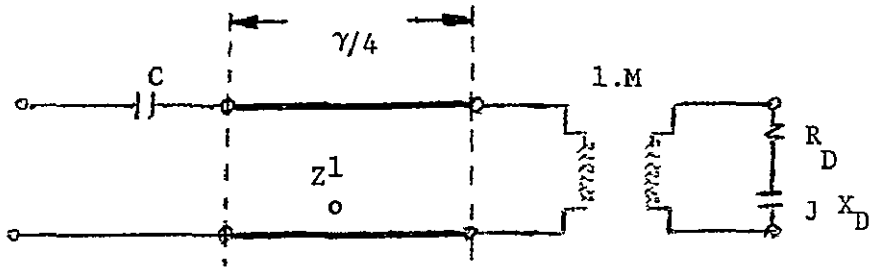

The dipole impedance is represented by R_D and X_D, the balance-to-unbalance impedance transformation is represented by the transformer with M = 2. The length of the three-wire line is approximately $\lambda/4$. The probe capacitance is C. For the impedance presented to the feed line to be pure resistive, of value R_2, the following conditions must be satisfied:

$$X_D = \frac{R_D}{WCR_2^2} \qquad Z_o^{1\,2} = \frac{R_2}{4}\left(1 + \frac{1}{W^2 C^2 R_2^2}\right)$$

The length of the dipole will be adjusted so that the first equation is satisfied. The characteristic impedance of the 3-wire line will be designed in accordance with the second equation.

The following set of values, while rough, are typical:

R_D = 70 ohms

R_2 = 1200 ohms

f = 1680 MHZ

X_D = 57 ohms, capacitive

Z_o = 22 ohms

C = 0.1 pf.

length/diameter ratio of dipoles = 20.

The main feed line will utilize air dielectric for the most part. Insulating spacers will be installed as dictated by rigidity requirements.

The mutual coupling of one dipole to its neighbor, and of one bay to the next, has been neglected. Experimental measurements will be resorted to, to uncover these effects.

4.4 FREQUENCY BEAM PROBLEM

At the NETCOS meeting on April 3, 1970, the transmit and receive frequency bands were identified as the following:

Bandwidtn:	20 MHZ for receive
	20 MHZ for transmit
Separation:	100 MHZ between band centers
Center Frequency.	1600 MHZ

The problem with beam position being a function of frequency (for the linear/array which feeds the parabolic cylinder), was immediately recognized. It was suggested a center-fed array instead of the end-fed one would eliminate the beam shift but, of course, would cause beam broadening, gain, loss, etc.

For an array with elements equally spaced, the angle δ that the beam makes, with respect to the broadside direction, is given by:

$$\sin = \frac{\psi_o \lambda}{2\pi d}$$

Here λ is the wavelength, d is the element spacing, and ψ_o is the phase of one element with respect to the adjacent element. For an array composed of pure shunt elements, with wavelength spacing, the phasing is

$$\psi_o = \frac{2\pi d}{\lambda} - 2\pi, \qquad d = \lambda_o$$

c

For the design frequency ($\lambda = \lambda_o$), the beam is accurately broadside. As the frequency is changed, ψ_o departs from zero, and the beam angle becomes

$$\delta = \frac{\lambda_o - \lambda}{\lambda}, \qquad \delta << 1.$$

$$= \frac{\Delta f}{f}$$

For a frequency change of 1%, the beam is scanned by 0.6°. For the present application, the transmit and receive bands are separated by about 6%, and the transmit and receive beams are separated by about 3.5° -- an intolerable amount.

If the array is fed in the middle, the beam from half the array scans in one direction while the beam from the opposite half of the array scans in the opposite direction. The resulting beam is thus maintained in the broadside direction, but is degraded in that the gain is lowered, the beamwidth is broadened, the sidelobes are worse, and the first null is filled in. To obtain an estimate of the amount of these effects, a pattern has been calculated. The elements spacing was chosen to be one wavelength, at 1600 MHZ.

If performance at one of the frequency bands were to be optimized, at the expense of the performance at the other frequency band, a different spacing could be chosen. However, since there is no preferred communication link at this time, both transmit and receive bands have been treated equally.

The results of the calculation are shown in Figure 4.5. The maximum field strengths are in the ratio 2.00:1.94. The antenna gain, for the center-fed array, relative to the gain for the end-fed case, is (1 + R) 2/4. Here R is the ratio of the two field strengths (2.00.1.94), and hence the change in gain is only 0.13 dB. As can be seen from the patterns of Figure 4.2, the beamwidths are about the same. The sharp null characteristics of the array with uniform amplitude and phase is filled in by the phase error associated with the center-fed array.

A second effect associated with the frequency scanning of the beam has to do with achieving the northerly bias of the beam (to make its center point toward the North Atlantic, rather than toward the equator). Originally, the tilt was achieved by making the element spacing a few percent different than a wavelength. Because of the frequency spread between the receive and transmit bands, this scheme would cause the two beams to point in different directions.

A suggested method of achieving the desired beam tilt (4°) is to make the axis of the reflector differ from the axis of the array by half the tilt angle (2°). The undesirable effect of this is to move the feed from the focal point, and hence deforms the antenna a small amount. The feed is displaced from the focal point a maximum of 0.673 inch at the ends of the array. This amounts to about $\lambda/10$, while the average deviation is about $\lambda/20$. The gain loss associated with this defocusing is estimated to be less than 0.2 dB.

PATTERNS OF END-FED AND CENTER-FED ARRAY
6 ELEMENTS
λ-SPACING (AT 1600 MHz)
ISOTROPIC ELEMENTS
END-FED
CENTER-FED
(1650 MHz
& 1550 MHz)
RELATIVE FIELD STRENGTH
ANGLE OFF PEAK OF BEAM (DEGREES)
HTW
9/13/70

Fig. 4.4

The revised gain estimate for the parabolic cylinder antenna is shown below:

Aperture Efficiency	97%
Spillover Efficiency	60
Phase Error Efficiency *	97
Defocusing Efficiency **	95
Miscellaneous Efficiency	90
Overall Efficiency	48.4%

$$\text{gain} = 48.4\% \text{ of } \frac{4\pi A}{\lambda^2} = 21.6 \text{ dB.}$$

---

* - Due to "frequency scan" effect

** - Due to beam tilt of 4°.

4.5 ANTENNA DRIVE

Although several suppliers and agencies have developed electro-mechanical antenna drive systems for various applications, none to date have had the NETCOS normal requirement of Earth's rate rotation, together with dynamic speed control for error correction at periodic intervals. In addition, in the backup spin control mode, the antenna drive must counter the vehicle spin rate of 1.0 rpm. Thus, the dynamic range of output speeds required for NETCOS antenna drive is 1,440 to 1 (6.95×10^{-4} rpm which is Earth's rate to 1.0 rpm in the failure mode).

Furthermore, the requirement for a fixed feed antenna (with only the reflector rotating to follow the Earth) means that the drive system must have a center aperture several inches in diameter, at least. Therefore the last

pass of a geared system would necessarily be a pinion engaging the outside of a large ring gear attached to the load.

Table 4-1 presents a summary of the characteristics of typical candidate systems, both geared and direct driven, including an indication of tne prior applications or flight status.

The Ball Brothers drive has limited angular freedon in both axes. The Sylvania and Philco-Ford drives run synchronously at 50 to 150 rpm -- too fast for use in NETCOS without further reduction gearing. Further speed reduction to 1 revolution per day means that several additional gear passes aggregating 144,000 to 1 would be required. The Hughes proposed system is servo driven by sun orientation error signals, and is not designed for continuous rotation. The Kearfott drive, with its output speed of 0.025 rpm, requires further reduction gearing of 36 to 1 to drive the load at Earth's rate. The Kearfott concept is for a very large solar array on the SIVB, and develops 125 ft-lb stall torque. This is an overdesign for NETCOS. A scaled-down version may appear more attractive.

Thus, none of the drive systems listed in Table is adequate for direct application to the NETCOS antenna drive. However, some combination of the USM Harmonid Drive components and a synchronous motor with good acceleration characteristics appears feasible. If a geared system were chosen, the dynamic speed change requirement may necessitate use of a differential gear and two motors. This type of drive is used on astronomical telescopes to drive them in right ascension at Earth's rate to follow a star. The fast speed input to the differential is used to slew the telescope to a desired initial setting. However, in geared systems, backlash control is only accomplished at the expense of increased friction torque. These considerations make the direct drive motor more attractive.

Table 4-1

Candidate Drive Subsystems

Supplier / Characteristic	United Shoe Machinery			Ball Brothers Res. Corp.	Sylvania/ TRW	Philco Ford S.R.S. Div.	Hughes S.S. Div. "OLSCA" (Orientat. Link. Solar Cell Array)	Kear-Fott/ Gen'l Prec./ Singer
	Direct		Geared					
	Pancake	Responsyn	(Flexspline harmonic)					
Motor	Multipole ≤ 82	8 pole stepper, 3 sizes	Any 0-3500 RPM NEMA "C"	Inland or Aeroflex DC	128 step 50-100 RPM Control Elect.	8 pole prs. Brushless DC 72-95rpm	DC Brushless	Inland T-4036F Brush DC (3)
Gear Ratio	No	≥ 200 per pass		No	No	No	No	100/1
Size/Weight	Large	Small/Light		10 lbs	Medium	10 lbs	---	7d x 12l 66 lbs.
Sealed	No	Optional		No	No	No	No	No
Lube	Brng only	Minimum Internal		BBRC Vac Kote	Evap. Lube, 50 yrs	Evap. Lube, 50 yrs.	Dry Lube	Molydisulfide
Speed Sensor	Pulse Rate	Optional		14 Bit Encoder	$\frac{360^{o}}{512}$ deg. Encoder	Mag. Pickup	Any	Inland TG-4014 Tach Gen.
Duty Cycle	0 - 100%			0-100%	0-100%	0-100%	0-100%	0-100%
Position Accurary (Backlash)	±.001% 12 sec	≥ 800 steps/ rev	2 to 6 arc min. at motor	±.05°	$0.7^{o} = \frac{360}{512}$	---	Servo sun sensors	---
Power	Hi	Hi	Low	3 w	21-31v .325 a	<5 w	---	90 w max
Status/Qualif.	---	200°F Temp. Vib., Shock, Rad., Vacuum 6000 hr life		Design Life 7 years	-100° + 120°F 6800 hr. vib. vacuum	5 year design life	Design Study 1968	Design Only, meets specs.
Application	Open Loop Servo for Space	Tape Dr; Valve	3 Pegasus Bell Stol, Radar, Lox Valve S-V Mech	OSO I- IV despin, Aerobee 60 units	ATS-III Intel. III despin	U.K. Satellite Despin	A.F. Study	S-IVB Solar Array for NASA/ MSFC
Angular Freedom	360°	360°	360°	± 20°	360°	360°	360°	360°
Max Speed Output RPM	VARIOUS			110	150	110	---	.025

Direct-driven, unsealed, multipole types of drive are most attractive for reasons of simplicity and reliability, but suffer from relatively high power consumption and weight. Geared drives employing relatively high-speed synchronous motor present low weight and power but suffer because of high load reflected inertia, very high gear ratios (up to 2.59 million for an 1800 rpm motor), as well as lubrication and wear problems. Nevertheless, these problems are minimized in the unique USM Harmonic Drive.

Geared systems, such as the Harmonic Drive giving up to 200/1 per gear pass, would require at least 3 passes in the Earth's rate leg of the drive, and perhaps only 1 in the slewing leg.

The speed change problem appears to be most easily solved by varying the frequency of the multipole motor and using a normally-off electronically actuated brake on the load to save power at the low duty cycle required when driving the antenna at Earth's rate.

The advantages of USM's* direct antenna drive for the NETCOS antenna are.

1) No gearing
2) Can be accelerated with high torque
3) Dynamic braking when reverting to low speed.

*United Shoe Machinery - Schaeffer Magnetics Div., Chatsworth, Col.

The multipole hysterisis synchronous motor would be driven by 2 very low frequency sinusoidally varying (not square wave pulses) AC voltages at 90° phase shift. All pole pairs are energized at once.

A power supply would need development. A problem is the very low frequency.

A simulation was conducted at Schaeffer Electronics using a 24 pole motor and 2 DC voltages varied manually in polarity and amplitude. About 3 watts was used, but this would be increased in actual application, depending on maximum torque required.

Schaeffer has delivered to Sylvania for Comsat a motor with the following chacteristics.

64 poles

7" diameter bore (clear hole)

Torque: 25 oz-in

Power. 6 watts input

Weight: 3-1/2 pounds

Synchronous speed. 80 rpm

Studies are continuing to further define the performance, flight status, reliability and physical characteristics of the various candidate drive subsystems leading to a selection of the best one for the NETCOS application.

5.0 MASS PROPERTIES *

The NETCOS weight and inertia study was conducted under the specification that weight be a minimum and that the spacecraft centroidal longitudinal to lateral inertia ratios be a maximum. The study is presupposed to be a conservative one necessary for a preliminary definition and analysis of the spacecraft. Basic engineering weight and inertial models characterize this study. It was assumed throughout that the location of the center of burn of the apogee motor fuel with respect to the separation plane defined the spacecraft center of gravity and that all expendable fuel items were located about this point. In the case of the module equipment inertia the longitudinal inertia was maximized to an optimum.

Table 5-10 presents the inertia breakdown with $\bar{y}$ defining each component's location with respect to the separation plane, I_o, defining each component's principal inertia, and d, the distance between the component and the spacecraft center of gravity.

*Updated Mass Properties appear in Appendix B.

5.1 WEIGHT BREAKDOWN TABLES

The following Tables present a weight summary (Table 5-1) and the weight breakdown of each of the systems included in the summary (Table 5-2 thru Table 5-9).

Table 5.1 Weight Summary

Item	Weight (lbs)
Power System	182.30
TM & Command System	23.00
Communication System	75.98
Antenna System	9.22
Stabilization and Control System	49.90
Auxiliary Propulsion System*	72.70
Thermal Control System	15.00
Electrical Distribution System	30.00
Structure	68.17
Apogee Motor Inerts (at burn-out)	46.40
Weight Growth Margin	87.95
Total Payload	660.60
Apogee Motor Propellant**	594.40
Adaptor	45.00
Gross Weight	1300.00

*Includes 2.1 pounds propellant expended during transfer orbit

** Includes 5.4 pounds of low performance expendable "inerts"

Stabilization and Control System

Item	Weight (lbs)
Electronics	6
Inertia Wheel	30
Attitude Determination	11
Passive Damper	2.9
	49.9

Table 5-2

Auxiliary Propulsion System Weight

Item	Quantity	Weight (each) (lbs)	Weight (total) (lbs)
Propellant Tanks	4 (11.5" dia)	2.3	9.2
Propellant			
Attitude Control			17.1
Orbit Control			31.3
Pressurant			1.0
Fill and Drain Valve	2	.28	6
Pressure Transducers	2	.32	.6
Isolation Valve	4	.63	2.5
Thermocouple	2	.06	.1
Filter	2	.40	.8
Fitting and Lines		2.51	2.5
0.5 #F Thruster and Valve Assembly	10	.55	5.5
5.0 #F Thruster and Valve Assembly	2	.75	1.5
			72.7

Table 5-3

Power System Weight Summary
Single Module Configuration

Item	Quantity	Weight (each) lb	Weight (total) lb
Batteries	2	30.5	61.0
Solar Array Plus Deploy System (10 lb)			100
Battery Discharger Controller	2	8.0	16.0
Voltage Limiter	2	1.5	3.0
Bus Parallel Relay	1	0.3	0.3
Power System V & I T/M	1	1.0	1.0
Under Voltage Detection	2	0.5	1.0
Total			182.3

Table 5-4

Structure Weight Summary

Item	Weight (lbs)
Lower Frustum	9.11
Module Support Ring, Lower	1.80
Apogee Motor Ring	1.80
Module Support Ring, Upper	1.80
Cylinder	8.50
Module Structure	38.20
Module Equipment Mounting Hardware	3.00
Upper Frustum	1.70
Bearing, Inner and Outer Ring	2.26
Structure Total	68.17

Table 5-5

Communication System Weights

Communication System	Quantity	Weight (each) lbs	Weight (total) lbs	Size (inches)
C-Band TWT	2	0.94	1.88	
C-Band TWT Power Supply	2	1.35	2.70	
L-Band TWT	2	2.00	4.00	
L-Band TWT Power Supply	2	8.00	16.00	
L-Band Ant. Elec.	1	1.00	1.00	
C-Band Ant. Elec.	1	.50	.50	
MDA and Electronics				
Motor-fixed feed	1	8.00	8.00	
Drive Elect.	1	6.00	6.00	5x8x2.5
Narrow Band L-Band				
XMTR	1	2.5	2.5	4x8x1.5
Narrow Band L-Band				
Mode	1	1.0	1.0	8x6x5
C-L Band Rptr.	1	13.0	13.0	14x8x4
L-C Band Rptr.	1	13.0	13.0	14x8x4
RF Switches and Filters				
L-Band		4.4	4.4	
Diplexer	1	2.0	2.0	4x6x.5
		$\sum$ W	75.98	

Table 5-6

Table 5-7

Total Weight, Module Structure

Item	Weight (lbs)
Sides	13.8
Top and Bottom Skins	8.1
Top and Bottom Stiffeners	1.6
Edging Members	6.4
Bulkhead Frame Members	0.7
Bulkhead Webs	0.6
External Braces	1.0
Miscellaneous (inserts and hardware for assembling module structure)	6.0
ΣW	38.2 lbs

Table 5-8

Total Weight, Solar Array

Item	Weight (lbs)
Cell Stack Weight	36.30
Thermal Paint	6.65
Structure	
Faces	17.40
Glueline	14.50
Core	10.40
Deployment System	10.00
Hinges	1.20
Edging Members	3.54
ΣW	99.99 lbs

Table 5-9

Total Weight, Antenna System

Item	Weight (lbs)
Antenna	4.62
Antenna Feed	1.26
Antenna Reflector	.34
Antenna Support Structure	3.00
ΣW	9.22 lbs

5.2 MASS MOMENT OF INERTIA

Inertia List, 1200 Watt Concept

Component	W lb	$\bar{y}$ in	Io_{xx} lb in^2	Io_{yy} lb in^2	Io_{zz} lb in^2	d in	d^2 in^2	wd^2 lb in^2
Lower Frustum	9 11	9 5	1,789	2,959	1,789	22 77	518	4,720
Mod Sup Ring, Lwr	1 8	20 27	95	380	95	12	144	259
Apog Mtr Ring	1 8	33 0	95	380	95	73	533	96
Mod Sup Ring, Upr	1 8	44 27	95	380	95	12	144	259
Cylinder	8 5	32 27	1,302	1,789	1,302	0	0	0
Module Struc	38 2	32.27	13,270	31,900	26,400	0	0	0
Module Equip (1)	280 38	27 26	60,870	244,673	186,907	5	25	7,000
Antenna Sup Str	3	59 78	55 4	60 51	55 4	27 51	756	2,268
Bear, In & Out Ring	2 26	54 78	74 7	299	74 7	22 5	506	1,142
Antenna	4 62	83 78	972	1,540	845	51 5	2,658	12,280
Antenna Feed	1 26	83 78	109	2 83	109	51 5	2,658	3,340
Ant Reflector	34	83 78	41 6	4 8	45 3	51 5	2,658	904
Propell Tanks								
Full	61 5	32 27	13,006	25,256	13,006	0	0	0
Empty	31 2	32 27	6,478	12,628	6,478	0	0	0
Fuel Apog Mtr	594 4	32 27	41,850	42,860	41,850	0	0	0
Apog Mtr Inerts	46 6	27 25	9,770	4,117	9,770	5 02	-	1,141
Solar Array								
Stowed	100	30 07	74,400	76,250	58,100	2 2	4 84	484
Deployed	100	30 07	1,149,000	1,120,000	28,000	2 2	4.84	484
Upper Frustum	1 7	48 93	122	216	122	16 66	278	472
Jets not considered	5 5	-----	-----	-----	-----		-----	-----
Mounting hardware not considered 3 pounds								

$$\bar{Y} = \frac{\Sigma \bar{y}\, W}{\Sigma W} = \frac{37338.65}{1157.07} = 32.27 \qquad \Sigma W d^2 = 34269.96$$

Stowed.

$I_{cg_{xx}}$ = 252,186.7 lb in^2 = (54.4 slug ft^2)

$I_{cg_{yy}}$ = 433,067 14 lb in^2 = (93.4 slug ft^2)

$I_{cg_{zz}}$ = 374,930 4 lb in^2 = (80.9 slug ft^2)

$\left(\frac{I_{yy}}{I_{xx}}\right)'$ = 1.72 y/x , $\left(\frac{I_{yy}}{I_{zz}}\right)$ = 1 15 y/z

Deployed

$I_{cg_{xx}}$ = 1,278,408.7 lb in^2 = (275.7 slug ft^2)

$I_{cg_{yy}}$ = 1,421,329 14 lb in^2 = (306.5 slug ft^2)

$I_{cg_{zz}}$ = 269.182 4 lb in^2 = (58.1 slug ft^2)

$\left(\frac{I_{yy}}{I_{xx}}\right)$ = 1 11 y/x , $\left(\frac{I_{yy}}{I_{zz}}\right)$ = 5.30 y/z

Table 5-10

Table 5-10 (con't)

NOTES·

(1)

Module Equipment Includes

Item	Weight (lb)
Power System less Solar Array	82.30
TM and Command System	23.00
Stabilization and Control System	47.00
Thermal Control System	15.00
Electrical Distribution System	30.00
Communication System less Antenna, Feed and Reflector	75.98
Auxiliary Propulsion System less Jets, Propellants Tanks and Associated Fuel	7.10
Total	280.38

6.0 ATTITUDE AND ORBIT CONTROL

6.1 MISSION SEQUENCE, OPERATION AND REQUIREMENTS SUMMARY

The launch vehicle is assumed to be the Delta 904 with a seven foot fairing. The ascent trajectory consists of a near East launch from ETR, into essentially a 100 n. mi. parking orbit, and injection at the second equatorial crossing into a 28.5-degree inclined transfer orbit to synchronous altitude. Injection into the desired synchronous, near equatorial circular orbit occurs at first apogee at about 90° West longitude some 6.4 hours after lift off. Alternatively, injection into the transfer orbit can be effected at the first equatorial crossing in the parking orbit. Injection at second apogee of the transfer orbit some 16.9 hours after lift off also yields a favorable injection longitude of about 53 degrees West.

The subject launch vehicle can inject a total payload of 1300 pounds into the indicated transfer orbit. A spacecraft adaptor comprises about 45 pounds of this weight.

The spacecraft will be separated from the spinning third stage of the Delta while in the attitude required for the transfer orbit injection maneuver. A partial spin down from 90 rpm to about 45 rpm will then be effected (to reduce subsequent precession control propellant requirements), using a side-mounted, outward-firing jet couple located near the plane of the spacecraft CG. Thereafter, spin stabilization will be used for attitude control during the transfer orbit and during the synchronous orbit injection and initial correction maneuvers.

A 127-degree yaw precession of the separated, spinning spacecraft is next accomplished by ground command to orient it as required for the apogee injection maneuver. Asymmetric pulsing of one thruster from the central pair of diametrically opposed thrusters, with thrust axes parallel to the spin axis will be used for this purpose (Figure 6-1).

The apogee injection stage must provide a velocity impulse of 6030 ft./sec. to accomplish the indicated apogee maneuver. Following injection into the synchronous near-equatorial orbit and identification of any existing period/eccentricity injection errors, initial orbit correction maneuvers can be accomplished. By thus making the indicated initial period and eccentricity correction maneuvers (coordinated so as to reduce the required velocity impulse) as soon as possible while still spinning, unwanted satellite eastward/westward drifts relative to the earth can be minimized.

No North-South stationkeeping will be provided during the planned mission to compensate for inclination perturbations. Hence, correction of the expected small initial inclination errors is not warranted (a relatively large velocity impulse would be required), and an initial inclination bias of several degrees can probably be used to center the inclination "drift" changes about a near zero value.

The indicated "spin axis" precession control thrusters can be employed for the ground based orbit correction maneuvers, using asymmetric thrusting of one thruster to precess the spinning spacecraft to the proper orientation and symmetric thrusting of the pair of diametrically opposed thrusters to provide the required corrective velocity impulse. Propellant requirements have been sized to cover a full 360-degree precession maneuver and

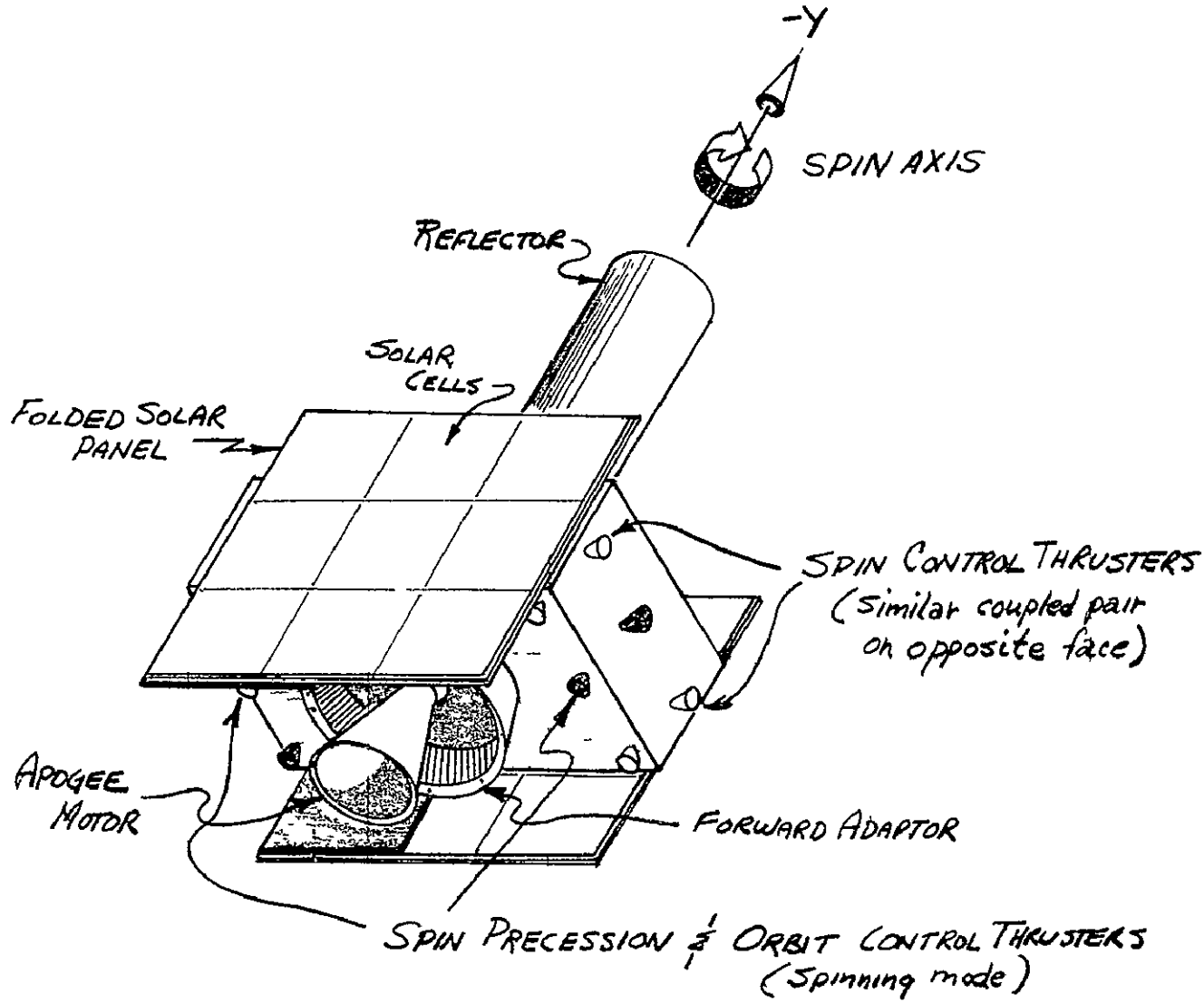

FIG 6-1 STOWED SPINNING NETCOS CONFIGURATION

a corrective velocity impulse of 300 ft./sec. This impulse is a very conservative value compared to the expected inplane injection errors.

Orbit corrections could also be provided during the spinning mode by appropriately pulsing one or both of the central pair of radial-firing, side mounted thrusters (Figure 6-1). Associated disturbance torques would be acceptably small since the thrust vectors of these jets can be closely aligned with the spacecraft CG for both the stowed and deployed configurations.

Orbit corrections can be made following deployment and acquisition of the sun-referenced attitude using these same jets These thrusters are also used for East-West stationkeeping and station relocation maneuvers as later discussed.

Following initial synchronous orbit correction maneuvers, the spacecraft will be despun using the previously indicated side-mounted jet (couple) lying near the plane of the spacecraft CG. The solar panels will next be unfolded. Three-axis jet torqueing will then be provided by means of the thrusters aligned with the original spin (y) axis and the side-mounted jets for torqueing about this y axis (Figure 6-2). These thrusters are used for ground command acquisition of the reference sun-oriented attitude also as shown in Figure 6-2.

It was noted that the spacecraft layout will be planned so that the plane of the side-mounted jets will closely coincide with the CG of the stowed fully loaded and of the deployed, apogee-motor-expended spacecraft Further, the solar panels will be positioned so that the total average center of pressure of the deployed spacecraft will be very close to the deployed spacecraft CG. This will minimize the steady solar pressure disturbance torque

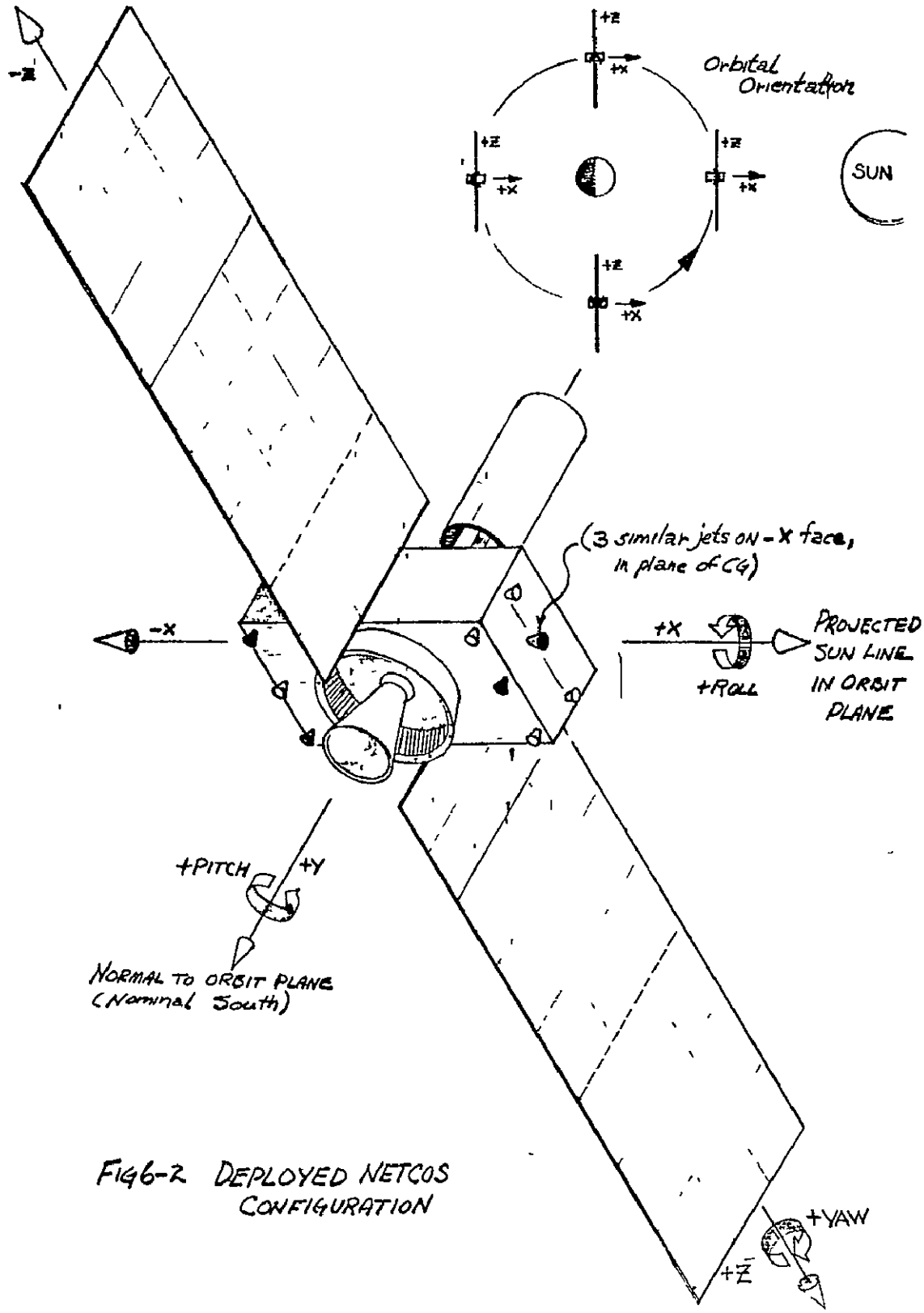

FIG 6-2 DEPLOYED NETCOS CONFIGURATION

acting on the spacecraft, leaving periodically varying torques about the y/z axes due to the varying solar aspect of the earth tracking antenna. An inertially-fixed bias torque will exist due to CP-CG uncertainty, this can be increased (or decreased) at solstice conditions due to a bias torque introduced by the sun illuminated top or bottom of the spacecraft.

Following acquisition of the reference orientation (original spin y axis of the spacecraft normal to the orbit plane and the x axis aligned to the sunline projection in the orbit plane), the momentum wheel aligned with the y axis will be accelerated to its bias speed. The jet thrusters will be used to counter the associated reaction torque on the spacecraft.

Reference to Figures 6-2 and 6-3 provides an indication of the attitude control approach envisioned for the normal operational mode. This includes pitch/yaw stabilization of the solar panels normal to the orbit plane and to the projected sunline and pitch stabilization of the antenna to a near-fixed earth orientation. It is noted that the expected orbit inclination variations of the NATS (up to ±2 degrees over its 5-year mission) will introduce a figure "8" pattern into its antenna ground aim point, with latitude excursion proportional to the inclination magnitude.

The near-constant-speed pitch momentum wheel will be used to provide gyroscopic stability of the satellite about its x/z axes in the orbit plane. The major requirement for this gyro stiffness is that it must stabilize against the dominant solar pressure and gravity gradient disturbance torques to an accuracy of about 0.5 degree between ground-originated, precession correction commands every 1 or 2 days. Roll attitude data are obtained at opposite sides of the orbit near the terminator plane, using two (redundant) earth sensors

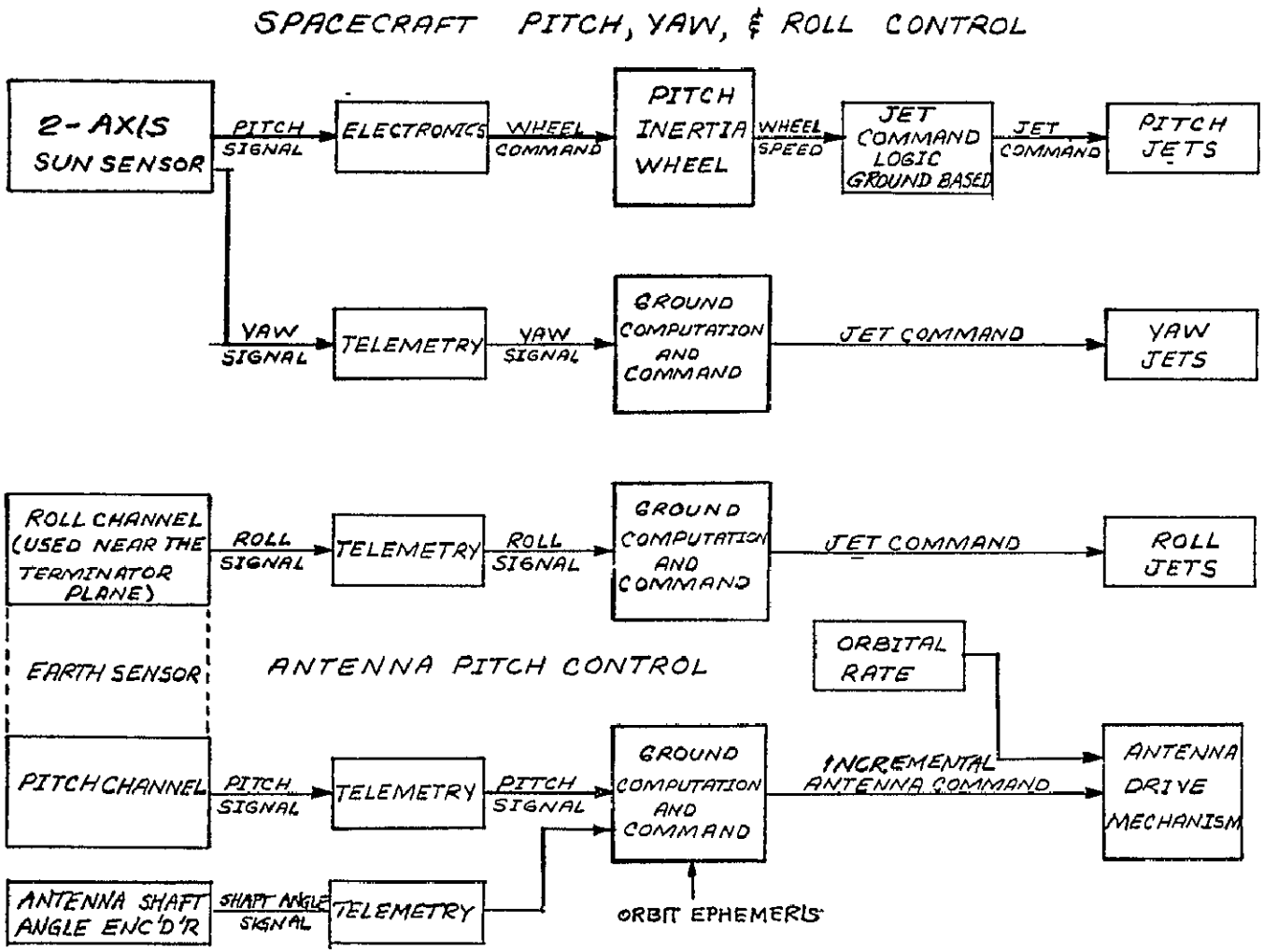

FIGURE 6-3, ATTITUDE CONTROL BLOCK DIAGRAM

looking out the ±z sides of the satellite. Jet pulse commands can then be used for corrective precession of the y (wheel spin) axis in roll, based on this earth sensor data, as telemetered to the ground.

Pitch angle data from this sensor (together with antenna shaft angle and orbit position - sunline data) can also be used to generate pitch correction commands to the antenna drive system. By adding these incremental commands every 1 - 2 days to the preset, constant orbit rate signal for the antenna drive system, the antenna can be caused to track its earth aim point to the desired 0.5-degree accuracy.

A similarly infrequent corrective precession of the y axis in yaw (about the z axis) can be effected by ground commanded jet firings, based on telemetered data from a wide-angle, 2-axis sun sensor looking along the +x axis of the spacecraft. (This same sun sensor is used to provide solar aspect data for attitude determination in the spin mode.) For this purpose, sun angle data on the sunline relative to the x axis in the x-z plane must be provided over a transverse angle range of about ±26 degrees (sunline relative to the x axis in the x-y plane). This North-South cross angle range is needed in order to accommodate summer/winter solstice conditions.

Since no gyroscopic stability is provided in pitch (around the y axis), it is envisioned that on-board, closed loop nulling of pitch error signals from the same 2-axis sun sensor will be provided. Limited up-down accelerations of the inertia wheel (still preserving a minimum bias speed by infrequent, ground commanded jet firings if necessary) can be used for this purpose to minimize limit cycle motions and propellant expenditures.

Propellant for an East-West stationkeeping velocity impulse of 35 ft./sec. (7 ft./sec. per year for 5 years) and a station relocation impulse of 25 ft./sec. is provided. The center, side-mounted thrusters aimed through the CG and parallel to the x axis are used for this purpose. These maneuvers must be accomplished near the terminator plane for the thrust vector to be effectively parallel to the spacecraft velocity vector.

In sizing the propellant tanks, a 50 percent contingency was added to the calculated attitude control propellant requirements for spin and for sun-referenced control. The latter includes stabilization against the dominant solar pressure disturbance torque for 5 years.

In order to improve mission reliability, backup redundancy has been provided for the attitude control sensors and torquers and for the orbit control thrusters for both the spin and sun-oriented operational control modes. In addition, a backup degraded-performance, spin-stabilized operational control mode is to be provided in the event of a failure of the y axis momentum wheel. The satellite would thus be spun at 1 rpm about its spin stable y axis (maximum moment of inertia for both the stowed and deployed configurations). The drive rate on the antenna would be increased from one revolution per day to 1 rpm in order to continue tracking the earth. The average solar power from the solar panels, now rotating around an axis normal to the orbit plane, would be correspondingly reduced.

6.2 APOGEE MOTOR

The apogee motor must provide a velocity impulse of 6030 ft./sec. in order to inject the spinning NETCOS into a synchronous, equatorial orbit. This maneuver is accomplished at apogee of the 28.5-degree inclined transfer orbit with a perigee altitude of 100 n. mi. and an apogee altitude of 19,323 n. mi. Actually, the velocity impulse can be reduced if an initial inclination bias of 2 degrees is employed in order to bias the inclination drift due to orbital perturbations about a near zero value. However, the full velocity impulse has been conservatively assumed for this study.

The apogee motor considered for this application is a modified Thiokol TE-M-442 motor with a 1.85 inch belly band (for the 1255 lb. design). This motor is predicted to have an exapended case weight of 46.4 pounds, a propellant specific impulse of 295.4 sec., and low performance expendables weighing 5.35 pounds with a specific impulse of 80 seconds.

The start-burn weight for the apogee maneuver is taken to be 1300 pounds (the assumed payload capability of the improved Delta launch vehicle into the indicated transfer orbit) minus 45 pounds (the aft spacecraft adapter which remains with the launch vehicle). Accordingly, the weight of the high performance propellant required for the apogee maneuver is 489 pounds. The total propellant weight, including low performance expendables, is thus 594.4 pounds.

6.3 ATTITUDE CONTROL SYSTEM (ACS)

6.3.1 Overall ACS

6.3.1.1 General

There are four different attitude control modes which must be considered:

- Spin control, employed during the transfer orbit, the apogee injection maneuver and the initial synchronous orbit correction maneuvers.
- Acquisition, employed during acquisition of the reference sun-oriented attitude.
- Operational, employed throughout the assumed 5-year mission in synchronous orbit to preserve the reference sun-oriented attitude.
- Backup Operational Spin Control, employed as a degraded performance control mode in synchronous orbit in the event of a failure of the momentum wheel used for 2-axis gyroscopic stabilization in the operational mode.

Most of the attitude control system (ACS) analysis to date has dealt with the operational mode as being the most critical. However, conceptual approaches have been defined for the other control modes which will also be briefly described in the following material.

6.3.1.2 Spin Control Mode

A basic constraint placed upon the spacecraft design is that its spin moment of inertia while stowed (solar panels folded) be greater than

its transverse moment of inertia by at least 10 percent. Hence, the spacecraft represents a stable spinning body while in the stowed condition Spin stabilization of the satellite is accordingly simplified and long term control in this mode can be provided (from several days up to a month or more).

Adequate electrical power for all spacecraft housekeeping functions is generated by the solar cells on the one outward-facing, stowed solar panel as long as the spin axis is maintained reasonably orthogonal to the sunline. The batteries can also meet this power requirement for a fairly extended period of time in the absence of solar power.

When the NETCOS is separated from the Delta 3rd stage, it will be spinning at rates up to 70-90 rpm. The despin thrusters (couple) shown in Figure 6-1 will be ground commanded to reduce the spin rate to about 45 rpm. This spin rate will still provide adequate spin stabilization against all disturbance torques, whether caused by natural sources or spin-thrust axis misalignments during the apogee maneuver. By thus lowering the spin rate, propellant requirements for the various spin precession maneuvers are reduced, as are spin acceleration loadings on the spacecraft during the apogee maneuver.

Use of the conventional sun sensor - Polang approach is anticipated for spin axis attitude determination on the ground. This method was employed for the early ATS vehicles and other satellites. Telemetered data from a wide angle (±30 degrees), 2-axis sun sensor looking along the +x axis of the spacecraft is used in this mode, together with a polarized antenna signal. This is the same sun sensor that is used for 2-axis solar aspect angle data for the subsequent acquisition and operational control modes.

Spin axis precession control as needed (e.g., to reorient the apogee motor thrust axis to the attitude required for the apogee maneuver) is accomplished by ground originated commands to one of the two (redundant) spin precession control thrusters shown in Figure 6-1. Use of a 0 5 $pound_F$ catalyzed hydrazine thruster for this purpose yields a fully adequate 0.1 deg/sec. precession rate and permits a flight proven thruster design to be chosen.

Initial synchronous orbit correction maneuvers, for quick elimination of period errors causing unwanted satellite longitude drifts, can be effected by ground command firing of both of these diametrically opposed thrusters. Spin precession commands would first be sent from the ground so as to orient their thrust axes in the required inertial direction for the corrective maneuver.

It is noted that orbit correction maneuvers can also be made in the spinning mode (and also following satellite despin and deployment and acquisition of the sun-oriented reference attitude) by ground command firing (at the appropriate spacecraft attitude and/or orbit position) of either of the two central, side-mounted thrusters (Figure 6-2). These are mounted on the ±x sides of the spacecraft and are closely aligned with the spacecraft CG for both the stowed and deployed conditions.

A passive damper will be employed to damp coning motions during the spin control mode. This same damper can function quite effectively to damp coning motions induced during the operational/backup spin control mode

6.3.1.3 Acquisition Control Mode

Following injection into synchronous orbit and completion of any desired initial orbit correction maneuvers, the satellite will be despun using

the indicated spin control thrusters. The solar panels will then be deployed.

Three-axis jet torqueing can then be provided by means of the 0.5-pound$_F$ hydrazine thrusters located on the +y and the ±x sides of the spacecraft. (Section 6.4 describes the appropriate use of these thrusters for attitude control in some detail.)

General orientation of the +x side of the spacecraft towards the sun as desired can then be effected by ground command of the appropriate jets based on telemetered data on the output power level of the solar panels. Alternatively, coarse sun sensors located around the sides of the satellite can be used for this purpose.

Once the sun is brought within the field-of-view of the wide angle, 2-axis sun sensor looking along the +x axis of the spacecraft, final alignment of this axis to the sunline can be effected.

The orientation of the spacecraft about the sunline will then be determined as the spacecraft approaches the terminator plane. At this point in orbit, one of the two earth sensor looking out along the +z and -z axes will see the earth. The roll attitude of the spacecraft can then be corrected as needed and acquisition of the reference sun-oriented attitude completed. This reference orientation consists of the y axis normal to the orbit plane (+y nominally pointing south for an equatorial orbit) and the +x axis pointing along the sunline as projected in the orbit plane.

The momentum wheel will then be brought up to its bias, gyroscopic-stabilization speed of 1400 rpm and the operational control mode can be initiated. The hydrazine thrusters providing a torque couple about the y axis

are used to stabilize the spacecraft during wheel spinup On-board, closed-loop nulling of the y axis signal from the 2-axis sun sensor is employed to provide this stabilization.

6 3 1.4 Operational Control Mode

The primary attitude control requirements to be met during the operational control mode include the following.

- To maintain the reference sun-oriented attitude (y axis normal to the orbit plane and +x axis aligned to the projected sunline in this plane) with an accuracy of ±0.5 degree about all three body axes. (A North-South or East-West angle error of 0.5 degree corresponds to a latitude or longitude deviation of the ground aim point of 2.8 degree.)

- To maximize the ACS reliability for the projected 5 year mission lifetime by the use of flight proven components wherever possible and by standby or functional redundancy for critical elements subject to realistic weight and/or power constraints.

With regard to the second requirement, a particular point of emphasis in the ACS design evolution was to minimize the on board controller requirements and to assign critical control functions to the ground station (e.g , control of the attitude control jets) where possible. At the same time, reasonable operational command/control requirements on the ground control

station have been maintained. Thus, it is planned that systemmatic ground command control functions, such as jet commands to correct attitude errors, shall be required no oftener than every 1 - 2 days, less often if possible

In order to meet the overall control accuracy requirement, the sensor accuracy specification was taken to be 0.1 degree desired, 0.25 degree maximum. It has been previously noted that North-South station keeping is not planned for the subject preoperational NETCOS design because of the prohibitively large velocity impulses associated therewith. The orbit inclination can probably be initially biased so as to balance the inclination "drift" due to orbital perturbations about a near zero value. This should keep the satellite subpoint latitude excursions within ±2 - 3 degrees in the 24-hour figure "8" pattern about the central equatorial longitude station. It should be possible to keep longitude excursions much smaller, within ±0.1 to 0.2 degree.

The basic concept for the planned ACS operational control mode was described in Section 6.1, with a functional block diagram given in Figure 6-3. The key features are that the satellite is essentially inertially stabilized (sun-orbital plane) with the exception of the reflector which is single axis driven about the spacecraft y axis so as to track the earth. A large momentum wheel is employed with spin axis parallel to the satellite y axis. The natural gyroscopic stability provided by this wheel can counter the effects of x/z disturbance torques and maintain the y axis normal to the orbit plane as desired for periods of 1 ~ 2 days (without the need for corrective control action). See Section 6.3.1.6.

On-board closed-loop nulling of pitch angle errors about the y axis (+x axis off the projected sunline as detected by a 2-axis sun sensor)

is provided, with torqueing accomplished by small variations in the high (1400 rpm) bias speed of the momentum wheel.

Firing of the hydrazine reaction jets for attitude error corrective torqueing about any of the three body axis can only be accomplished by ground command, and is only necessary on an infrequent basis (every 1 - 2 days). For this purpose, pitch/yaw angle data from a wide angle, 2-axis sun sensor (bore-sighted along the +x axis) and roll/pitch angle data (near the terminator plane) from two 2-axis earth sensors essentially aligned along the ±z axes are telemetered to the ground. See Section 6.3.2 Pitch angle data from this same earth sensor, together with relative drive angle data for the reflector and satellite ephemeris/ sunline data are used to generate incremental corrective drive commands as required for the antenna to track the earth.

It is noted as discussed in Section 6.3.2.1 that other locations and configurations were considered for the earth sensor. However, the indicated approach provides adequate angle data for stabilization of the satellite and reflector and is the most reliable of the approaches considered. As discussed in Sections 6.3.1.7 and 6.3 2.1, indexing of the sensor so as to provide pitch angle data near a midnight orbit condition may be necessary to meet satellite control requirements in the umbra.

6.3.1.5 Backup Operational Control Mode

Standby redundant sensors and reaction thrusters (for 3-axis torqueing) have been provided for the operational mode in order to enhance mission reliability. However weight limitations essentially preclude the inclusion of a redundant unit for the heavy (30 pound) momentum wheel and drive electronics.

Preliminary control analyses have shown that it is not sensible to use jet-only control in the event of a failure of momentum wheel. These studies revealed that the propellant consumption rate would be excessive even if thrusters much smaller than the planned 0.5 $pound_F$ jets were employed. Also, ground command control of the jets, used for reliability reasons during the operational mode, would not be practical because of the short period between jet limit cycle firings (10 to 40 seconds). Hence, the on board controller would have to be made more complex than desired.

An alternative backup operational spin control mode has been defined for use should the momentum wheel fail. The satellite has been designed so that its y axis is the maximum moment of inertia axis after deployment of the solar panels (as well as while stowed). By spinning the satellite about this axis should the momentum wheel fail, a spin stable backup operational control mode is thus provided.

A vehicle spin rate of 0.28 rpm would yield a gyroscopic stability equivalent to that provided by the momentum wheel. Spin rates up to 1 rpm are being considered to provide added spin stability. Factors that will influence the allowable spin rate include the acceleration loadings on the deployed solar panels, the increase in antenna drive rate from the normal 1 revolution per day, and the scanning operation of the earth sensor. However, a spin rate of 1 rpm appears acceptable from all of these standpoints.

During the backup operational control mode, the ground command/control method for spin control would be essentially the same as that described for the initial spin control mode. The solar power available would be somewhat

less than half the full power associated with the sun-referenced operational mode. This is because of the 1 rpm rotation of the panels about the y axis (still maintained normal to the orbit plane).

6.3.1.6 Disturbance Torque Analysis

Disturbance torques acting on the NETCOS have been considered from three basic aspects for the operational control mode:

- The impact they have on sizing the momentum wheel so that it can provide inherent gyroscopic stabilization about the x-z axes to an accuracy of 0.5 degree for 1-2 days.
- The secular momentum buildup they may impart to the spacecraft about any axis which must be countered by the expenditure of reaction jet propellant, based on ground commands to the thrusters.
- The time varying momentum they may impart about the y axis which can be countered by variations in the momentum wheel bias speed, accomplished by on-board closed-loop nulling of pitch error signals from the 2-axis sun sensor.

The two dominant disturbance torques of concern for NETCOS arise from solar pressure and gravity gradient effects. The only significant gravity gradient torque is a sinusoidal one about the y axis with a period equal to one-half the orbital period. The maximum value for this torque (midway between the terminator plane and noon/midnight in orbit) is given by:

$$\left|\begin{matrix} T \\ y \end{matrix}\right| = \left(3/2\right) \omega_o^2 \left(I_x - I_z\right) = (1.5)\ (7.29 \times 10^{-5})^2\ (276 - 58)$$

$$= 1.73 \times 10^{-6} \text{ ft-lb}$$

With a spin axis moment of inertia of 0.0647 slug-ft^2 for the momentum wheel under consideration, only a small change in the wheel bias speed ($\Delta\omega$) is needed to compensate for this torque over one-half cycle (one fourth orbital period) Thus,

$$\Delta\omega(\text{rpm}) = \frac{(.707)\ (T_y)}{I} \left(\frac{15}{\omega_o}\right) = \frac{(.707)\ 3\ (I_x - I_z)\ \omega_o\ (15)}{2\ I}$$

$$= \frac{(15.9)\ (276-58)}{(0.0647)} \qquad (7.29 \times 10^{-5})$$

$$= 3.9 \text{ rpm}$$

Hence, the most critical disturbance torque for NETCOS is that caused by solar pressure as next discussed

The first R-F reflector considered for the solar pressure study was a parabolic unit tilted at an angle of 38 degrees with the x-y plane. The design approach was to consider the CG of the spacecraft fixed and to position the solar panels so that the resultant solar pressure moments were balanced for the equinox condition. This is shown in Figure 6-4a. A plot of the maximum roll angle excursion for this is shown in Figure 6-7. By starting at the initial sunrise condition with an appropriate 0.5 degree bias, it would be possible to obtain three orbit revolutions before a roll angle correction would be necessary The analysis procedure employed was similar to that given in Appendix A. A 0.5-inch fixed offset between the deployed CG and overall average center of pressure (CP) was used for these studies.

Due to the 38 degree tilt of the reflector, summer and winter solstice moments and resultant roll angles are appreciably more than those under equinox conditions and are not balanced. The moments are shown in Figures 6-4b

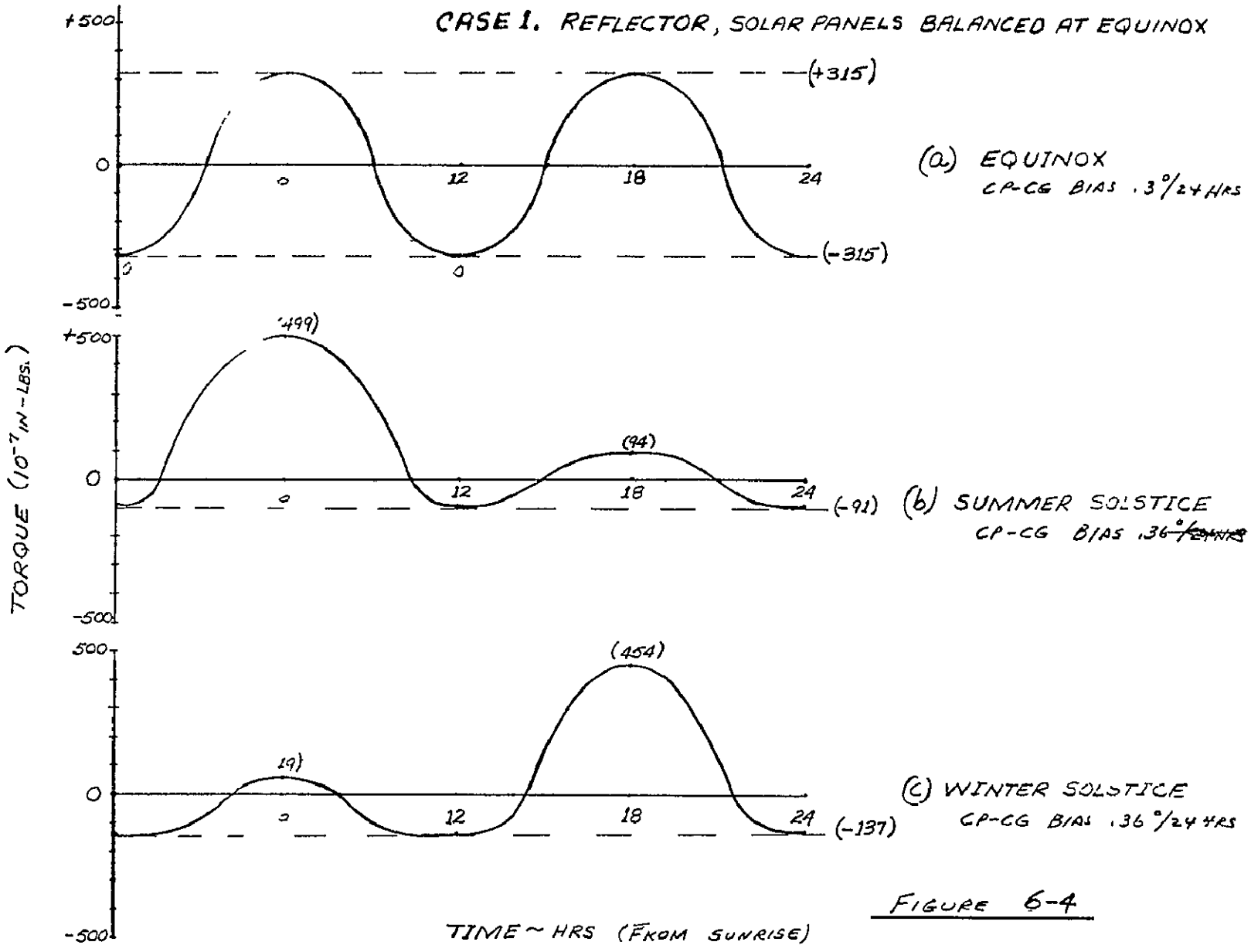
CASE 1. REFLECTOR, SOLAR PANELS BALANCED AT EQUINOX
+500
0
-500
(+315)
(-315)
0
12
18
24
(a) EQUINOX
CP-CG BIAS .3°/24 HRS
(499)
(94)
(-91)
(b) SUMMER SOLSTICE
CP-CG BIAS .36°/24 HRS
500
(454)
19)
(-137)
(c) WINTER SOLSTICE
CP-CG BIAS .36°/24 HRS
TORQUE (10^{-7} IN-LBS.)
TIME ~ HRS (FROM SUNRISE)

FIGURE 6-4

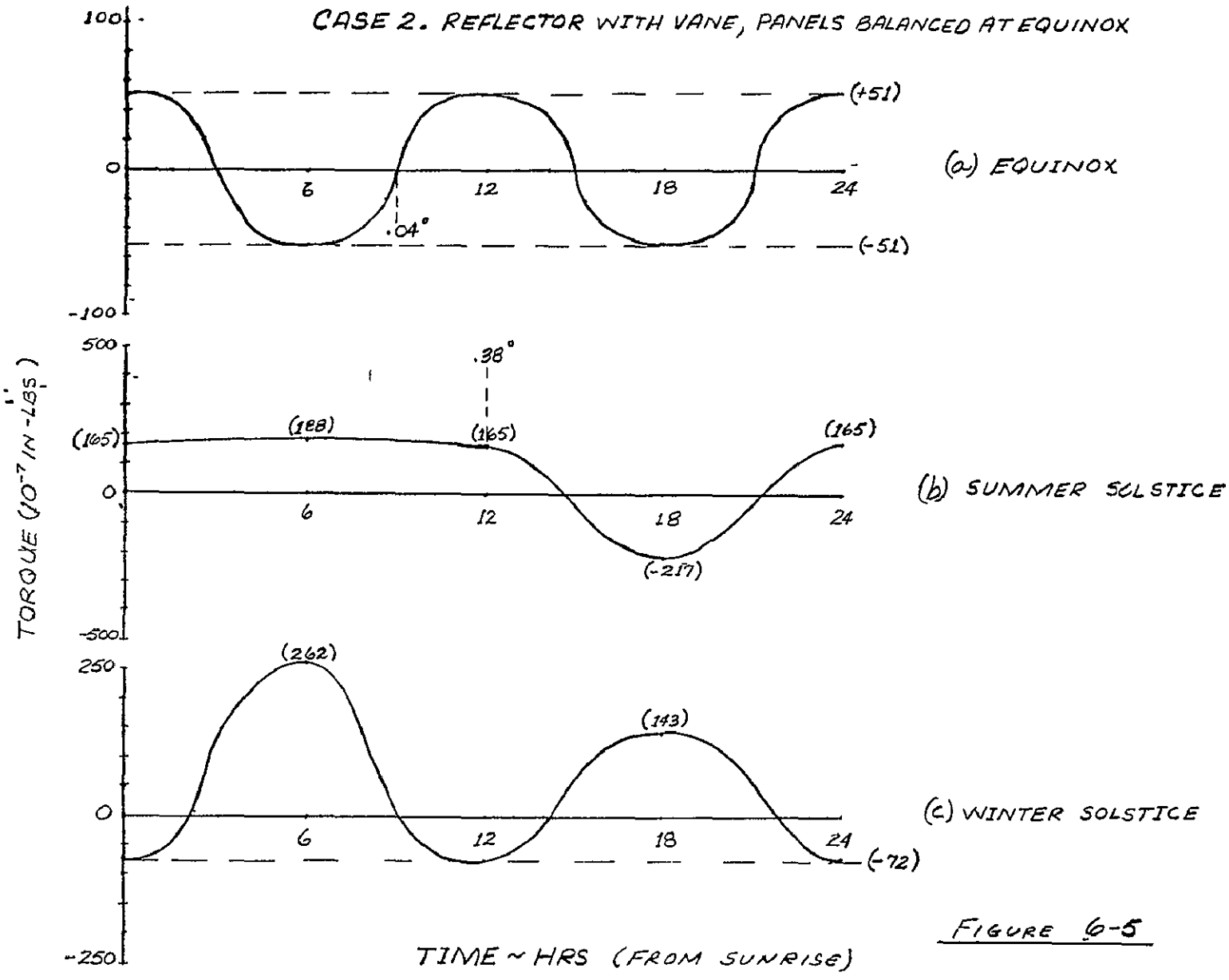
CASE 2. REFLECTOR WITH VANE, PANELS BALANCED AT EQUINOX
100
0
-100
(+51)
(-51)
.04°
6
12
18
24
(a) EQUINOX
500
0
-500
.38°
(165)
(188)
(165)
(165)
(-217)
(b) SUMMER SOLSTICE
250
0
-250
(262)
(143)
(-72)
(c) WINTER SOLSTICE
TORQUE (10^{-7} IN-LBS)
TIME ~ HRS (FROM SUNRISE)

FIGURE 6-5

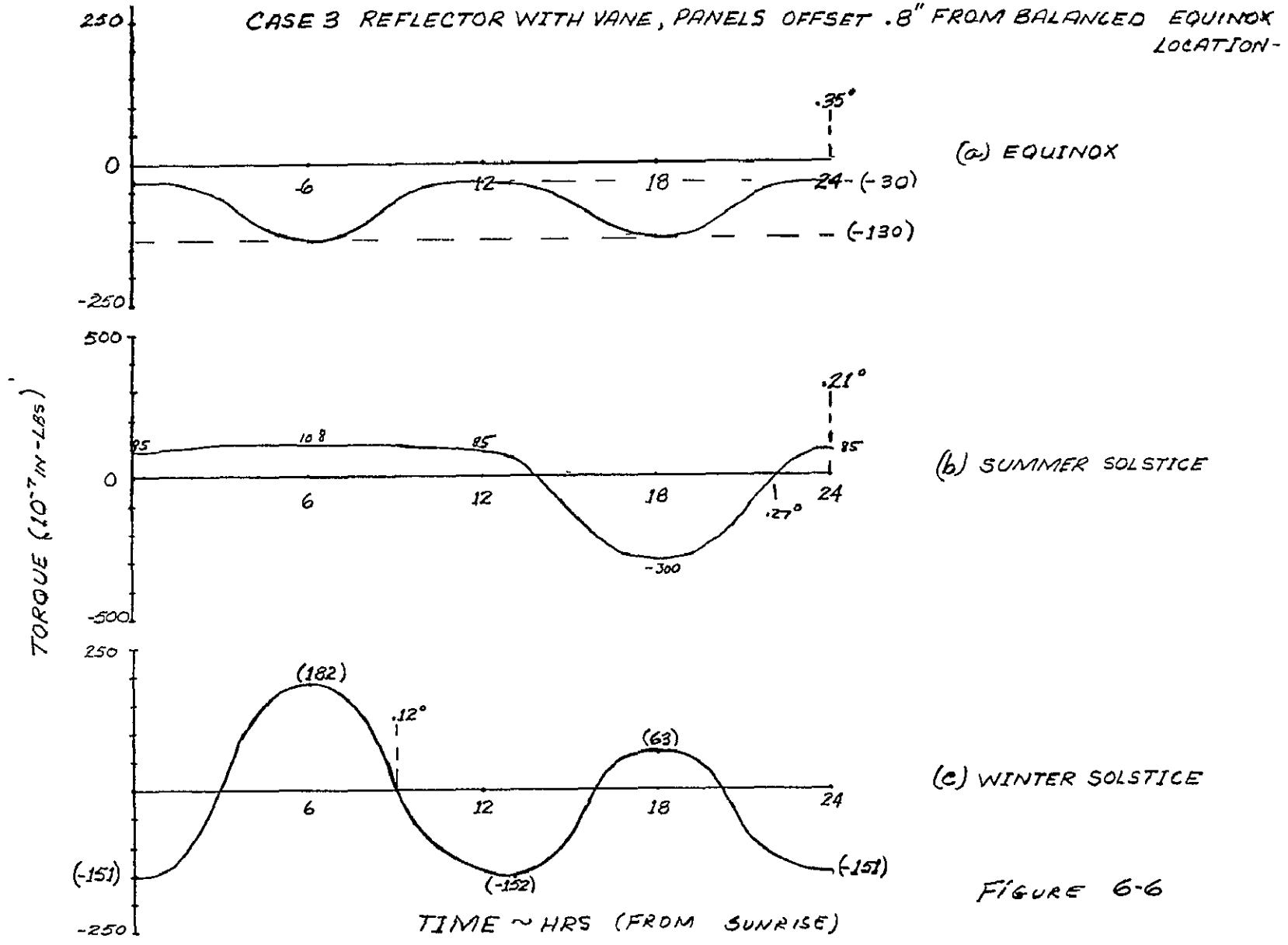
CASE 3 REFLECTOR WITH VANE, PANELS OFFSET .8" FROM BALANCED EQUINOX LOCATION-
250
0
-250
.35°
6
12
18
24
(-30)
(-130)
(a) EQUINOX
500
0
-500
.21°
95
108
85
95
6
12
18
24
.27°
-300
(b) SUMMER SOLSTICE
TORQUE (10⁻⁷ IN-LBS)
250
(182)
.12°
(63)
6
12
18
24
(-151)
(-152)
(-151)
-250
(c) WINTER SOLSTICE
TIME ~ HRS (FROM SUNRISE)

FIGURE 6-6

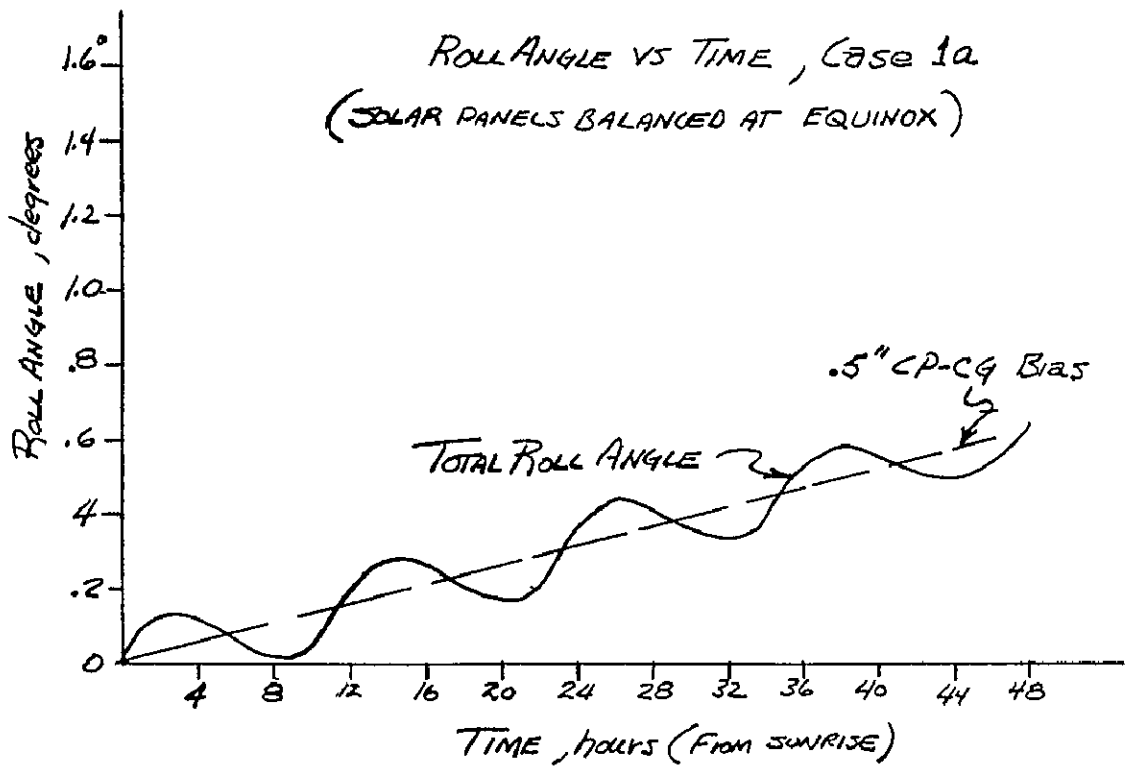
ROLL ANGLE VS TIME, Case 1a
(SOLAR PANELS BALANCED AT EQUINOX)
ROLL ANGLE, degrees
1.6°
1.4
1.2
1.0
.8
.6
.4
.2
0
.5" CP-CG Bias
TOTAL ROLL ANGLE
4
8
12
16
20
24
28
32
36
40
44
48
TIME, hours (FROM SUNRISE)

FIG. 6-7

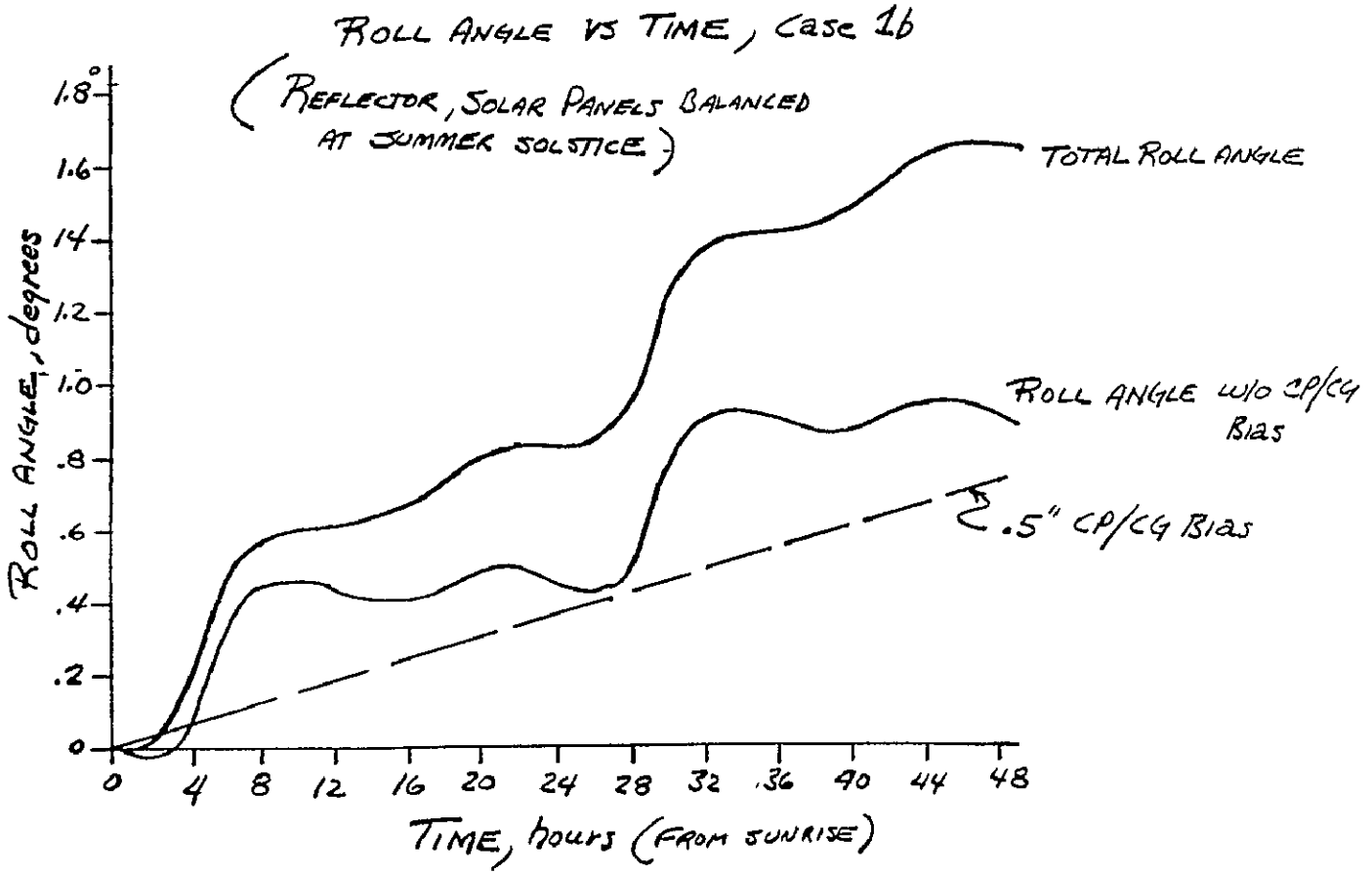
ROLL ANGLE VS TIME, Case 1b
(REFLECTOR, SOLAR PANELS BALANCED AT SUMMER SOLSTICE)
TOTAL ROLL ANGLE
ROLL ANGLE w/o CP/CG BIAS
.5" CP/CG BIAS
ROLL ANGLE, degrees
1.8°
1.6
1.4
1.2
1.0
.8
.6
.4
.2
0
0 4 8 12 16 20 24 28 32 36 40 44 48
TIME, hours (FROM SUNRISE)

Fig 6-8

and 6-4c and the maximum roll angle excursions are shown in Figure 6-8 for summer solstice. Winter solstice roll angles would be less than those for summer solstice. With the worst case for summer solstice one orbit revolution before roll correction is obtained by using an initial bias of 0.4 degree. If the CG-CP offset bias subtracts from the unbalanced periodic torque variation, then two or more revolutions without correction can be obtained.

In Figure 6-5 the moments are shown using a vane on the back of the reflector. The objective was to make the vane plus the reflector edge view look as much as possible like the reflector front view. This resulted in a low moment variation for equinox. However, solstice yields a large projected area due to the reflector tilt angle. Corrections once per orbit with an initial bias would be required for both summer and winter solstice when the CP-CG bias is additive to the periodic bias. The solar vane did not appear to improve the solstice conditions.

Case 3 shown in Figure 6-6 is the same as case 2 with the panels lowered 0.8 inch. Here again a correction once per orbit would be needed. There might be a more optimum panel shift not yet determined.

Calculations were next made for the rotating cylindrical parabolic antenna with a fixed feed as employed in the current NETCOS configuration. From a solar pressure standpoint this is superior to the tilted reflector.

Figure 6-9 shows the moment curves for this configuration. The curves show a smooth periodic variation for equinox and the solstices, offset slightly for summer solstice and a greater offset for winter solstice. Two orbits without correction can be accomplished at equinox and summer solstice. As plotted, two orbits cannot be achieved at winter solstice but a shift of the

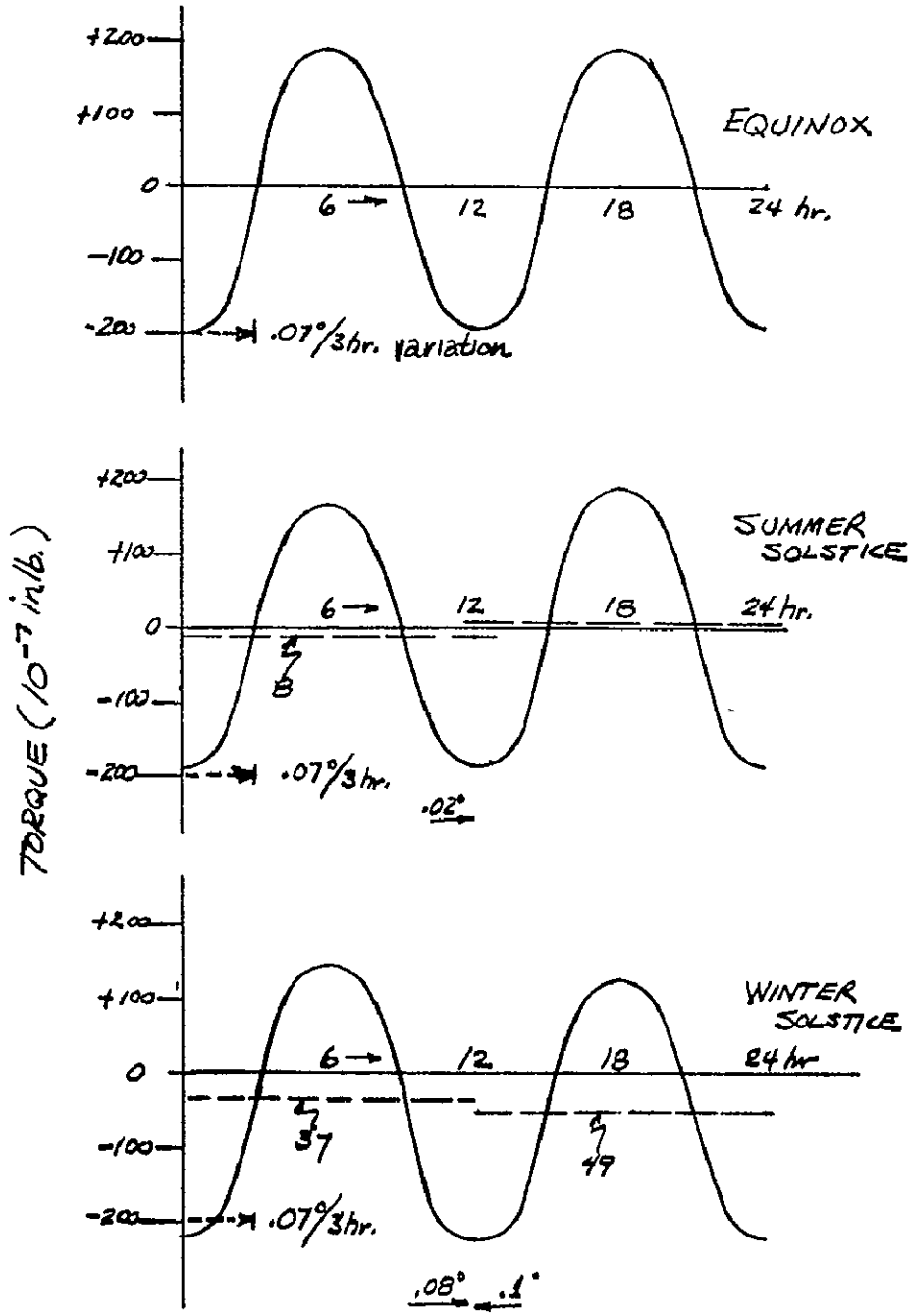

SOLAR PRESSURE TORQUES, ROTATING ANTENNA

FIG 6-9

solar panels will make it possible to achieve two orbits for winter solstice as well as the other two conditions.

The cyclic solar pressure component caused by the varying solar aspect of the reflector can also be reduced by using an open mesh reflector instead of the solid design assumed herein.

6 3.1.7 Umbra Control Analysis

Unique control problems arise when the NETCOS enters the umbra, or shadowed, portion of its orbit. In umbra, which lasts a maximum of approximately 70 minutes per orbit of a synchronous orbiting satellite during equinox (Figure 6-10), the effects of solar torque are absent and the gravity gradient torque is quite small. At midnight, which occurs in the middle of umbra, the gravity gradient torque is zero.

Due to this low torque condition during umbra, any impulses or disturbances imparted to the spacecraft just prior to entering the umbra could result in relatively large angular excursions about the spacecraft axes. For NETCOS, the momentum wheel provides gyroscopic stability about the spacecraft x and z axes. Therefore, there is no problem with excessive angular excursion in the umbra about these axes. However, there is no rigidity about the y axis (normal to the orbit plane) and control problems could arise for this axis.

A dynamic analysis was performed on NETCOS to study the possible control problems encountered within the umbra and to determine a feasible approach to the solution of these problems. Equinox was assumed to be representative of worst case conditions since the time the spacecraft spends in the umbra is then a maximum. It was also assumed that the maximum allowable control deadband about the y axis was ±0 5 degree (1 degree total).

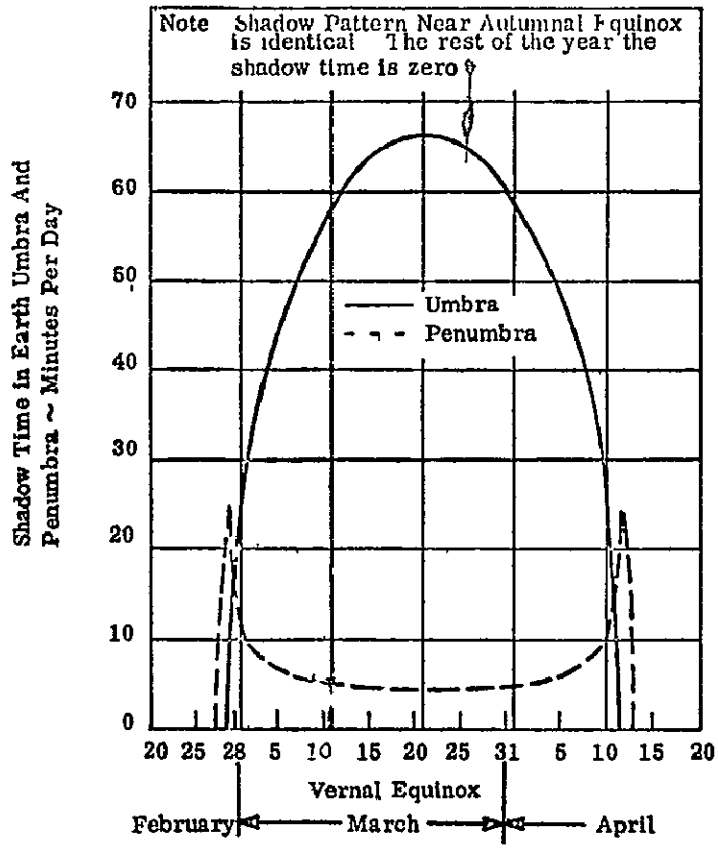

Figure 6-10 Umbra and Penumbra Patterns (Synchronous Equatorial Satellite)

The first step of this analysis was to determine the possible angular excursions about the wheel spin axis (spacecraft y axis) due to wheel speed changes as might be caused by windage and friction losses while in the umbra

Using the basic dynamic relationships

$$\Delta H = I_w \Delta \omega \qquad (1)$$

$$\Delta H = Tt \qquad (2)$$

$$T = I_{s/c} \alpha \qquad (3)$$

$$\theta = (1/2) \alpha t^2 \qquad (4)$$

where,

ΔH = change in momentum

I = y axis inertia (w-wheel, s/c-spacecraft)

t = time

$\Delta\omega$ = change in momentum wheel speed while in umbra

T = torque

α = angular acceleration

θ = angular excursion about spacecraft y axis

and assuming various values for $\Delta\omega$ (with an assumed linear buildup during umbra passage), a plot of θ versus time in the umbra was derived. From these results as presented in Figure 6-11, it was observed that for a $\Delta\omega$ of 1 rpm due to windage and friction losses in the umbra, θ is approximately 4 degrees (worst case). To keep θ within the desired deadband range of ±0.5 degrees, $\Delta\omega$ due to windage and friction losses in the umbra can be no greater than .1 rpm. This represents 0.007% of the assumed nominal wheel speed of 1400 rpm.

FIGURE 6-11

ANGULAR EXCURSION (θ) VS UMBRA PASSAGE TIME

(LINEAR WHEEL SPEED CHANGE)

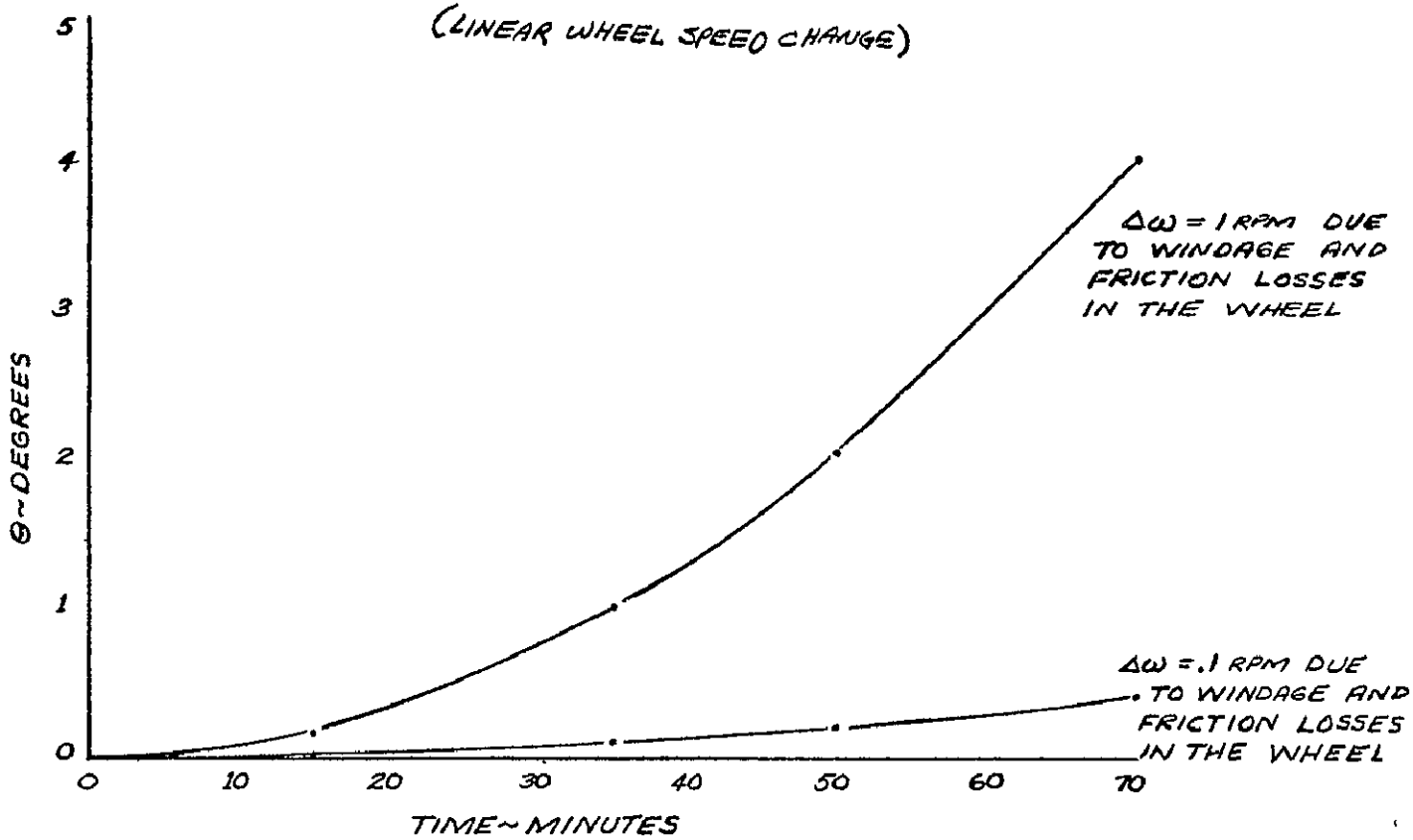

The next phase of the analysis was an investigation of the possible consequences of initiating a control action and causing a change in wheel speed ($\Delta\omega$) just prior to entering the umbra. It was assumed that there was no disturbance torque counteracting the momentum change of the wheel. Using the above-mentioned relationships, θ versus time in the umbra was plotted for various initial impulsive $\Delta\omega$ values, Figure 6-12. The results again display a need for very tight control of the inertia wheel. A $\Delta\omega$ of 1 rpm just prior to entering the maximum umbra with no disturbance torque results in a θ about the y-axis of over 8^{o}. A $\Delta\omega$ of .1 rpm results in a θ of $.8^{o}$.

A final portion of the control analysis dealt with the more general problem of the precision or resolution of wheel speed control required to ensure accurate limit cycle control for realizable disturbance torque levels. The torque levels considered ranged from a minimum value of 0.4×10^{-5} in-lb (corresponding to a near midnight/noon orbital condition, low solar pressure and gravity gradient torques) through an intermediate value of 1.11×10^{-5} (near sunrise/sunset condition, solar torque only), to a maximum value of 2.24×10^{-5} in-lb (midway between the foregoing conditions, near maximum solar pressure and gravity gradient torques).

A scallop limit cycle operation was assumed for this analysis as depicted in Figure 6-13. Using the same basic equations as before, the angular excursion (θ) about the spacecraft y axis which would accumulate during the time required for various torque levels to null the initial spacecraft rate caused by an initial impulsive change in wheel speed were calculated. These angle data are presented in Figures 6-14, together with a cross plot of the time required for the given torque levels to null the initial spacecraft rate caused by any given $\Delta\omega$ value. Separate plots of these time-to-null values versus $\Delta\omega$ for

FIGURE 6-12

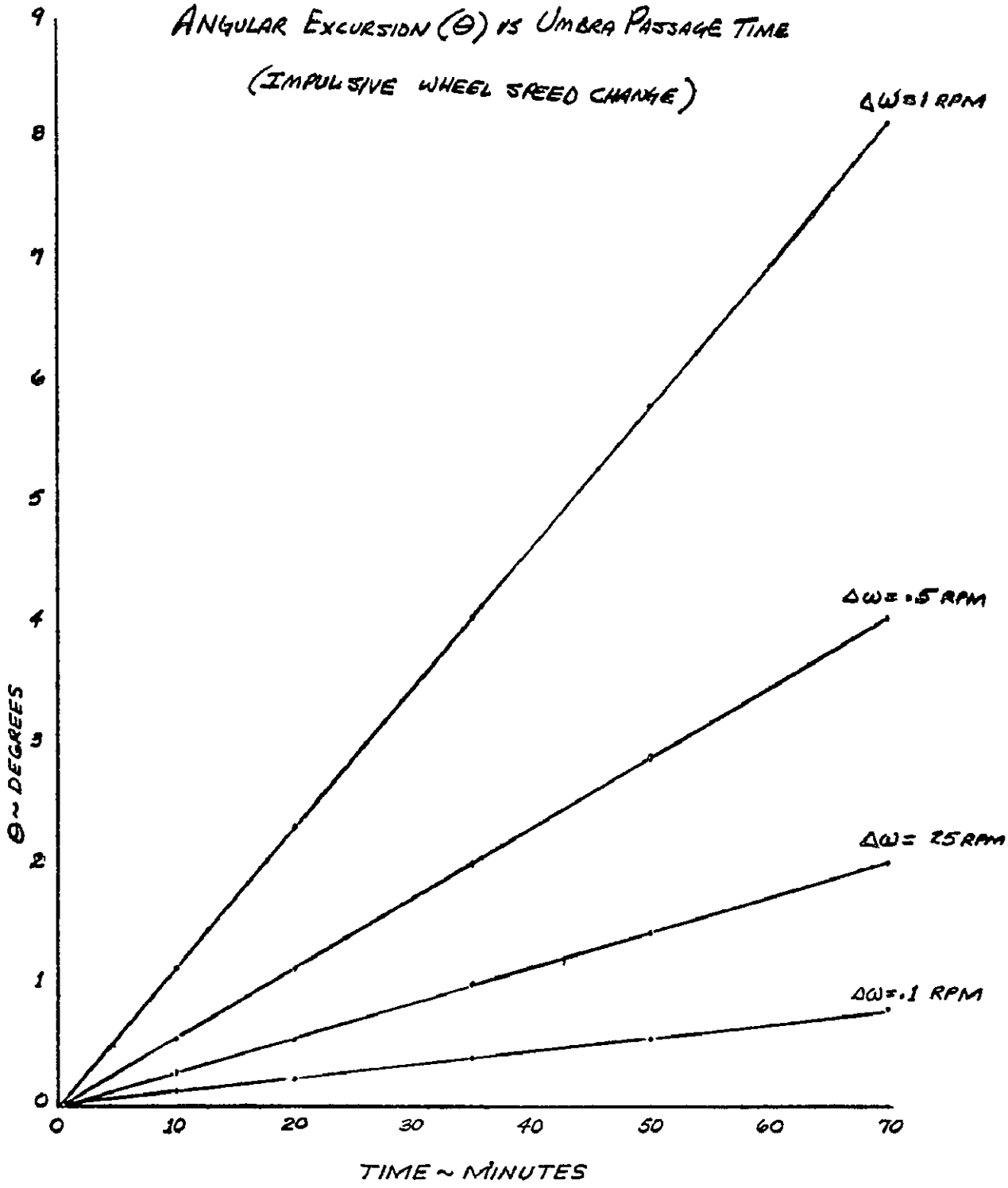
ANGULAR EXCURSION (θ) VS UMBRA PASSAGE TIME
(IMPULSIVE WHEEL SPEED CHANGE)
Δω=1 RPM
Δω=.5 RPM
Δω=.25 RPM
Δω=.1 RPM
θ ~ DEGREES
TIME ~ MINUTES
0
1
2
3
4
5
6
7
8
9
0
10
20
30
40
50
60
70

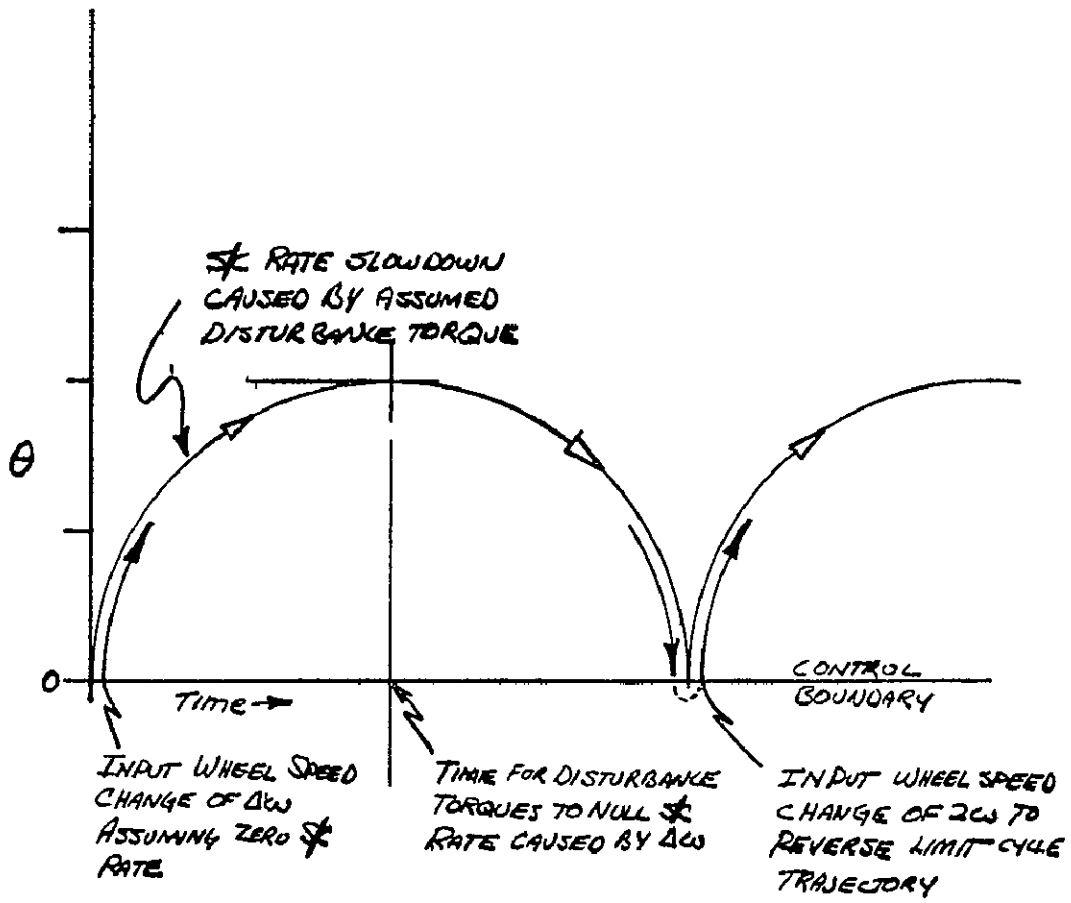

FIGURE 6-13. LIMIT CYCLE MODEL

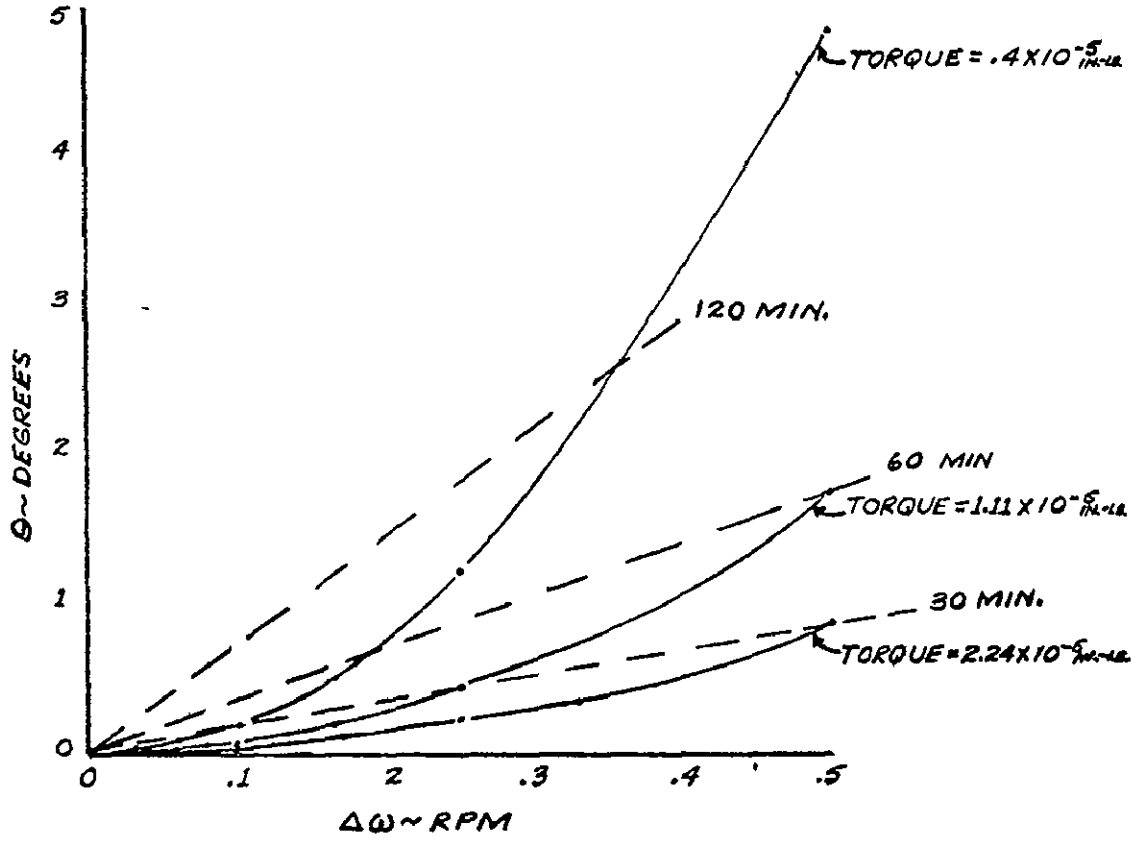

FIGURE 6-14. ANGULAR EXCURSION (θ)
vs.
WHEEL SPEED CHANGE (Δω)
(Zero SC Rate Before Δω)

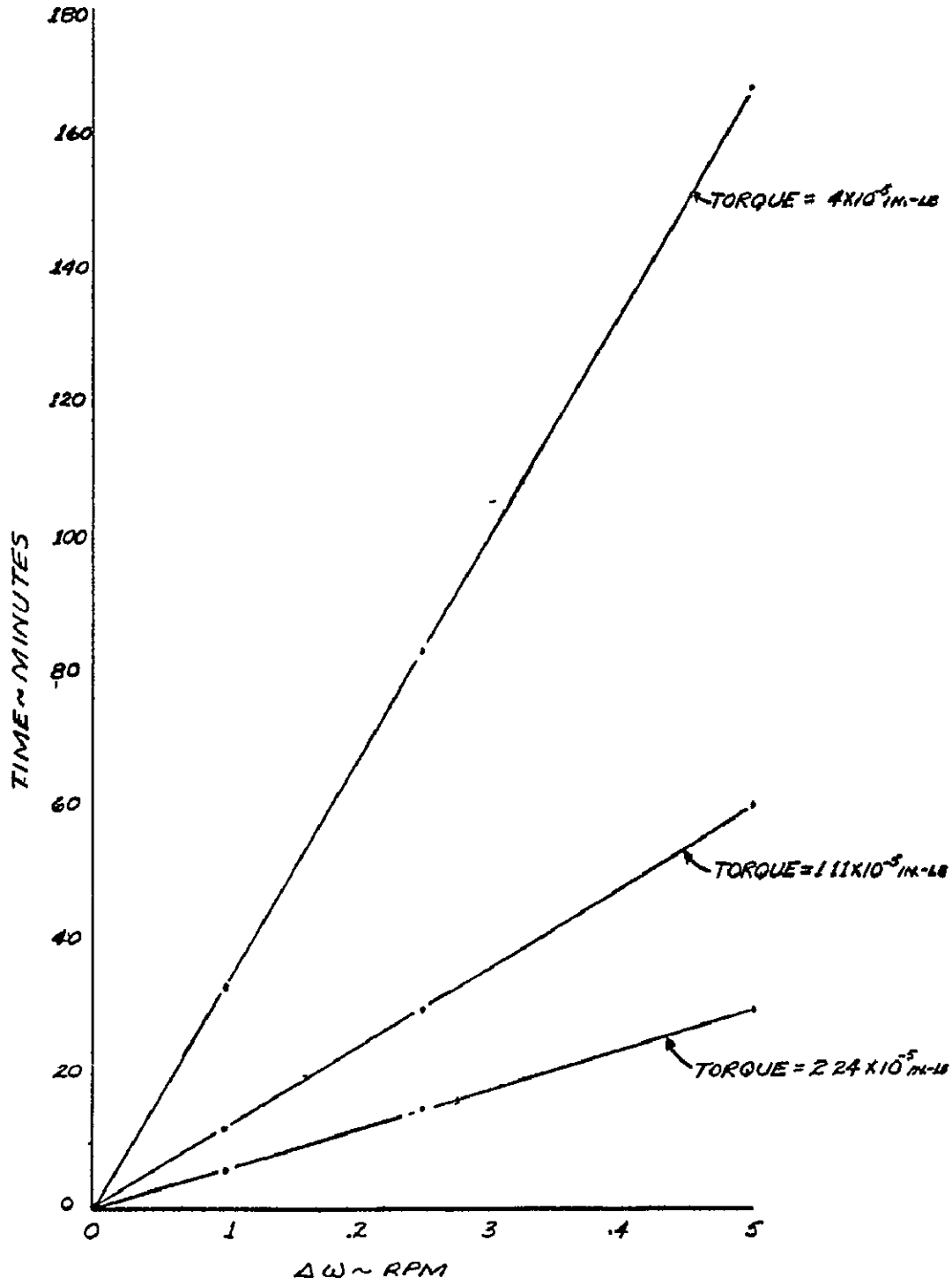

FIGURE 6-15. TIME TO NULL S/C RATE
vs.
WHEEL SPEED CHANGE
(Zero S/C Rate Before $\Delta\omega$)

various torque levels are also given in Figure 6-15.

It is noted that in a scallop limit cycle mode, as shown in Figure 6-13, the subject time-to-null would represent half the limit cycle period and the $\Delta\omega$ value would represent half the wheel speed change required at the crossing of the angle control boundary to reverse the limit cycle trajectory. This control impulse is provided at only one side of the angle control boundary for a scallop (soft) limit cycle, namely the side towards which the existing disturbance torque causes the spacecraft to drift.

Soft, scallop limit cycle control would result in lower wheel drive power requirements compared to a hard, two-boundary limit cycle control. However, the study results shown in Figure 6-14 indicate that in order to be able to realize soft limit cycle control, particularly at the lower disturbance torque levels, unrealistically fine speed control of the large momentum wheel would be required. Two solution possibilities can be considered:

- Operate in a hard limit cycle mode with correspondingly more frequent momentum wheel activations and higher average power requirements
- Provide a smaller, vernier reaction wheel for fine y axis control and utilize only fixed, preset wheel speed levels for the large momentum wheel, commanded in steps as necessary to prevent speed saturation of the small wheel.

Further studies are continuing on the relative advantages of these and other approaches.

With regard to the umbra control problem, subject to the outcome of current studies, it appears quite likely that closed loop control about the y axis will be necessary during umbra passage to prevent large angle excursions from developing. Since the two-axis sun sensor cannot be used for this purpose, consideration should be given to using the pitch signal from the earth sensor instead. The impact on the earth sensor location/design caused by this requirement for pitch data near a midnight orbit condition (in addition to the terminator plane positions previously required) are discussed in Section 6.3.2.1.

6.3.2 Sensors

As indicated previously, the sensors required for the various ACS control modes and for incremental antenna pointing corrections in pitch are:

- Two, 2-axis earth sensors (essentially redundant) looking nearly parallel to the +z and -z axes of the spacecraft
- Two, 2-axis wide angle sun sensors (fully redundant) boresighted along the +x axis of the spacecraft

A resolution/accuracy capability of 0.1 to 0.25 degree is required for each of these sensors. Summary data are next provided regarding candidate earth sensors and sun sensors.

6.3.2.1 Earth Sensor

Several existing earth sensors appear to be applicable for pitch and roll attitude determination for NETCOS. Their characteristics are summarized in Table 6-1, "Synchronous Orbit Earth Sensor Candidates." These are of two

Table 6-1

EARTH SENSOR CANDIDATES

	HONEYWELL	TRW	QUANTIC		LMSC	BARNES
DESIGNATION	DYG774A1	VELA/Visor	Static (no mirror)	IV A	NOHS Dual Scan (Null Op H S)	HAHS Earth-Lunar Modified (No Gimbals) (Hi Alt. H.S.)
TYPE	Radiation Balance	Scan Thru	Rad. Bal.	Rad. Bal Edge Trkr	Scan Thru 45^{o} Off Along Lats.	Rad. Bal, Edge Trkr.
MOVING PARTS	NO	YES 5 Hz	NO	YES Thermo-Static, Non Periodic	YES 4 Hz	NO
ACCURACY $\pm 3\sigma$	0.1^{o}	$<0.1^{o}$	$0\ 1^{o}$	0.03^{o}	0.017^{o} - 0.068^{o}	0.1^{o}
OUTPUT D - Digital A - Analog	A	A	A, 1v/deg or .5v/deg	A or D Ser/Par	D, $.01^{o}$/Digit A, 1v/deg	A, 1v/deg
LINEAR RANGE	$\pm 70^{o}$	$\pm 2.3^{o}$ min $\pm 19.3^{o}$ max	± 5 deg	± 10 deg	$\pm 10.24^{o}$ pitch $\pm 2.56^{o}$ roll	$\pm 0\ 5^{o}$ brk @ 1^{o} ± 10 deg Satura.
SPECTRUM MICRONS	11-20	14-17	22-40	14-16	14.1-15.8	13.7-16.3
AXES	2	1	2	2	2	2
WEIGHT, HD WEIGHT, ELEC. TOTAL WT.	6.5 — 6.5	~3.0 ~5.0 8.0	7.0 — 7 0	4(7)=28.0 10.0 38.0	4 0 — 4.0	2.0 — 2.0
VOL. HD. VOL ELEC. TOTAL VOL (cu. in)	30 95 125	~175 ~200 ~375	(8diax7) 350 — 350	4(116)=464 464+	(4 25x4.5x7.00) 134 — 134	(3diax7) 50 — 50
ALT. NM	100=60,000	Synch.	Synch.	80=26,000	Synch.	Synch.
POWER, watts	6.0	~7.0	2.2@ 22-31 vdc	22-34	5.0@28vdc	1.5@ 22-29.5vdc
SUN REJECTION	Acc ~0.25^{o}	Avoid	Avoid by Switching	Avoid by Switching	Pitch-Switches Roll-uses Std Chord	Avoid by Switching, Not inhibited
DETECTOR	Thermistor Bolometer (7)	Thermistor Bolometer (1)	Thermocouples (24)	(48)	Thermistor Bolometer (2)	Thermopiles (16)
REMARKS	Needs more development	In-Orbit 1967 Visor qual	Qual. for AF, ATS	Qual 30g sine, Life '66	Qual. design proof, life test compl.	Thermopiles qual. 35g -195+100C

general types: scanning and static radiometric. The static sensors (Quantic and Barnes) have no moving parts, but have conical fields of view. The scanners can be single-axis (TRW Vela) or two-axis (LMSC) configurations, and have fan-shaped planar fields of view.

To avoid a slip-ring and brush-block interface between an earth sensor mounted on the earth-oriented reflector and the sun-oriented satellite body, consideration was given at first to mounting the earth sensor in the satellite body, looking along the vehicle's pitch axis, and viewing the earth by reflection from a group of mirrors oriented 45 degrees with their input lines of sight parallel to the antenna axis. This approach was abandoned as it would have required resolution of the sensor signals from each mirror because of the exchange of the angle functions. Besides, prohibitively large flat mirrors would be required, mounted above the solar panel array, to accommodate the sensor's field of view which is necessarily always greater than 17.4 degrees, at synchronous altitudes.

For these reasons, the configuration shown in Figure 6-16 was chosen. Two two-axis earth sensors are installed behind the solar array as shown at A and B. Pitch and roll attitude determination is accomplished twice a day, near the terminator plane. To avoid placing a 3rd earth sensor at C in Figure 6-16 for attitude determination at midnight when the satellite is in the umbra, sensor B may be indexed 90° once a day to the position B^{1} for this purpose, by ground command.

Figure 6-17 shows how the single scanning mirror of a typical sensor scans the earth in a north-south direction. The Lockheed sensor, for instance, derives pitch and roll angle information as shown in this figure.

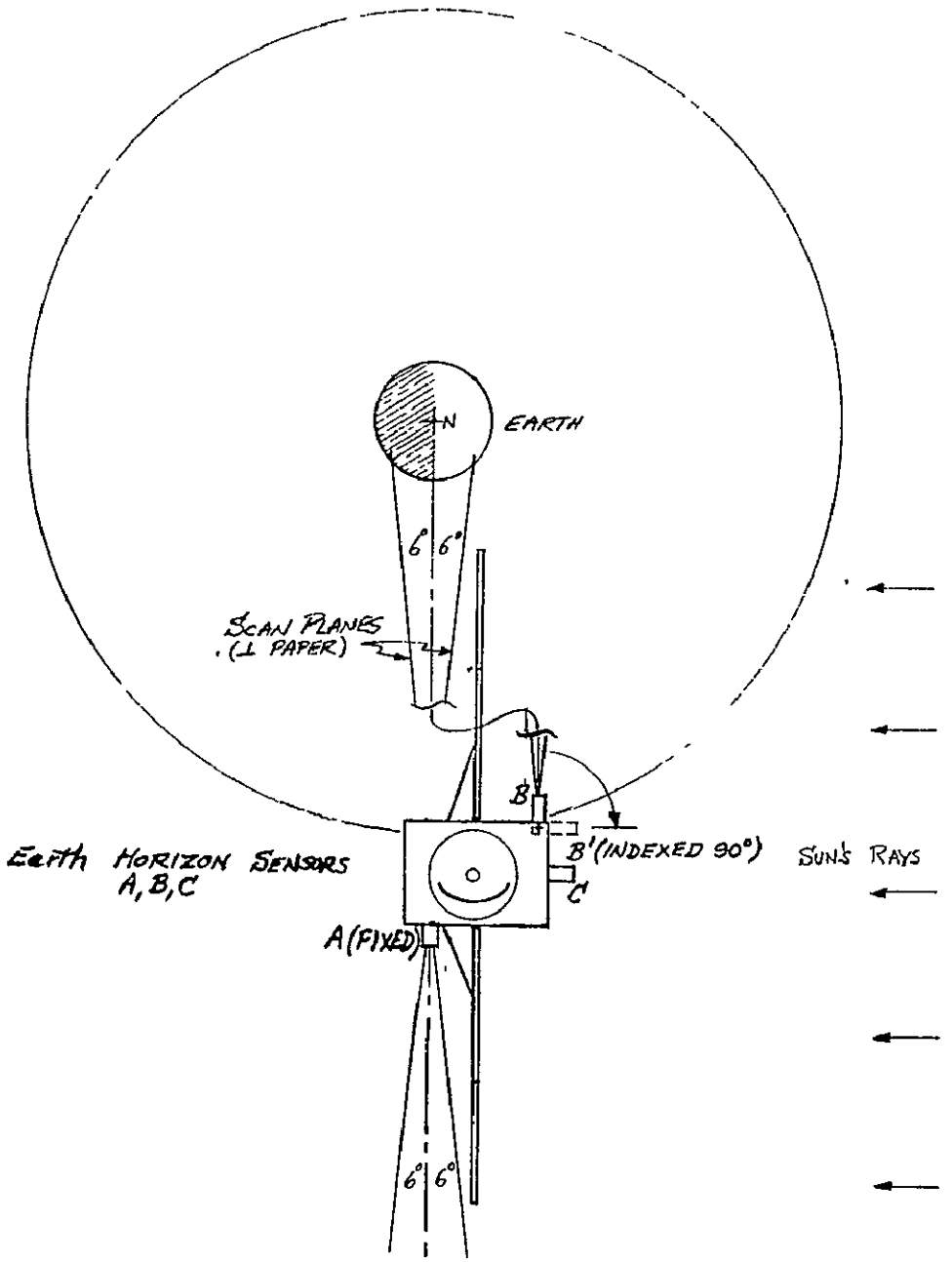

Figure 6-16

EARTH SENSOR INSTALLATION

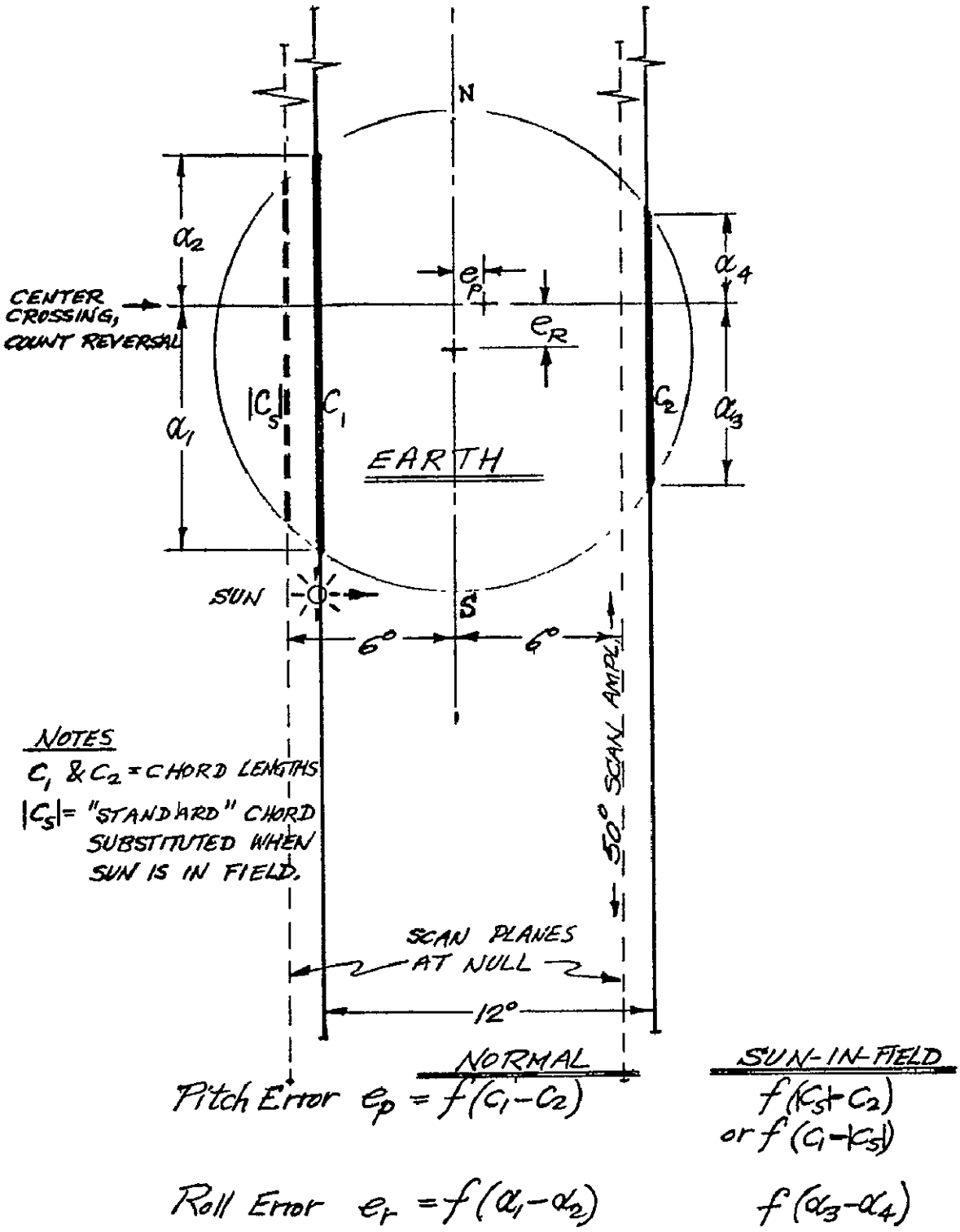

FIGURE 6-17 LMSC "NOHS" SCAN GEOMETRY

Pitch attitude (in this orientation of the sensor) is determined by computation of the sensed difference between two earth chord lengths which are separated by 12 degrees. Roll attitude is derived by timing the horizon-to-center crossing in each direction along one chord. Though not required for this configuration, sun avoidance capability in one form or another is provided for all the sensors considered. In the pitch axis, the Lockheed sensor substitutes a "standard" chord electrically for that chord in the scan plane intercepting the sun. Roll information is then derived by timing horizon crossings in the other scan plane, out of the sun's view.

It should be noted that use of the LMSC earth sensor here for illustrative purposes does not signify final selection of that sensor at this time, but the derivation of two-axis information from a single scanning mirror makes this concept attractive from a weight and power point of view. The NETCOS attitude control system weight budget reflects the assumed use of 2 LMSC earth sensors, at 4 pounds each.

6.3.2.2 Two-Axis Sun Sensors

A wide-field, two-axis solar aspect sensor with a resolution/ accuracy of 0.1 to 0.25 degree is required for NETCOS. It is planned to use this sensor for all of the basic control modes (spin, acquisition, operational and backup operational). The wide field in a plane normal to the orbit is necessary for account for the sun's annual excursion in declination, amounting to ±23.5 degrees, and for several degrees of orbital inclination. The total field of view requirement is thus ±26.5 degrees minimum, but a safe margin is provided by ±30 degrees.

In the orbital plane the field-of-view (FOV) requirements are narrower, about ±5 degrees, for all but the acquisition mode where a ±30 degree FOV is desirable. Also, if symmetrical optics and detector are used, the same size field is easily available in both axes. Special types of cylindrical optics would be necessary to deliverately narrow a field of view to a rectangular shape and still maintain a linear range in both axes.

Table 6-2 lists several types of wide-field sun sensors (both analog and digital) with appropriate associated performance and physical characteristics. All of these sensors are passive, strapped down devices with no moving parts. All use silicon photovoltaic cells which peak near0.8 micron wavelength, just outside the visible range. Response time is of the order of 5 to 20 microseconds. The favored EOS and BBRC candidate sensors appear capable of meeting this weight limit, including their processing electronics.

Budgeted weight for the optics, detector, and associated electronics for 2 (redundant) 2-axis sensors is 3 pounds maximum. The Electro Optical Systems Inc. Radiation Tracking Transducers (RTT) are designed for mechanical attachment to any "standard" lens such as the wide-field PAXAR identified in the table. However, the narrower the field (e.g., 60° instead of 180°) the better the resolution capability of the system.

TRW Systems Inc. also builds sun sensors for many aerospace programs. However, their analog sensors use the EOS RTT which is described herein.

6.3.3 Torquers

The torquers employed for attitude control of the NETCOS include reaction jets which are used for torqueing about all axes during the spin,

Table 6-2

Sun Sensor Candidates
For NETCOS

Supplier	Bendix		Ball Bros.	E.O.S		Adcole	
Type	Wide Field Sun Seeker	Binary Output Sun Sensor	Fine Sun Sensor Assembly	RTT (Detectors)		Solar Aspect Sensors/ Electronics	
Model No.	1771858	1771982	SS 100	XY20B	XY20E	10941/ 235	11974/ 11962
Characteristic	*	*					
Analog/Digital	An.	Dig.	An.	An.	An.	Dig.	Dig.
Sensitive Axes	2	2	2	2	2	1	2
Total Wt., lb.	19		~.68	~ 5**	~.5**	2 26	2.8
Size	1.9"dia. x 20"	~1.5"dia. x 6"	2.8" x 1.7x 1.8	2.62" dia. max. x ~2.7" lg.		see below, detector and electronics	
Power, watts	.005		~1.0	no electr.		.27	---
Linearity over Angular Range	5% ±10°	NA NA	~1% ±5	2% 8% @.025" 8% @.100"		--- ---	--- ---
Resolution, Noise	inf.	NA	inf	~inf .003°	~inf. .003°	0.5°	0.5°
Optics	Glass Cover	Mask Only	Glass Cover	No Optics Supplied		Internal	
Field of View	180°	(to order)	30°	±.225" ± 100" max	± .225" ± .025" useful	±32° x 2°	±64° x ± 64°
Size dia x lg.	1 7/8" x2"	NA	NA	Above are detector dimensions: F.O.V. depends on lens		NA	NA
Detector	Quad. 2/axis	----	Quad. 2/axis	1 →		#10941	#11974
Type	Silicon		Silicon	Silicon →		Silicon	
Signal gradient	1.8 max / deg.	---	35 μa/min 5 " "	25 mv/ mw/.001 in.		NA	NA
Size	Included in integrated package			1.2" dia x .9" lg		2@ 1.2" x 1.7" x .9"	3.2" x 3.2" x.6"
Weight	(.19 lb)		(0.38 lb)	.06 lb →		2@.13 lb	.5 lb
Electronics	Not Supplied		2 diff amp. + 4 amp + pwr. sup.	Not Supplied		#235 2 req.	#11962
Size			3" x 3" x 2"			2 req. 4.6" x 2.0 x 3.3"	6.5" x 4.5" x 2.3"
Weight			(~0.3 lb)			2@ 1.0	2.3 lb

* Detector only

** With 180° PAC "Paxar Periphoto" f/6.3, 2.62 dia x 1.75 lg lens, .35 lb plus housing

acquisition, operational and backup operational control modes and a momentum wheel used for gyroscopic stability about two axis and limited torqueing about the third axis during the operational mode. The configuration and operation of the jets are described in detail in Sections 6.1 and 6.4. The intended use of the momentum wheel is discussed in Sections 6.1 and 6.3.1.4. The characteristics of the proven momentum wheel design being considered for this application are summarized in Table 6-3.

6.3.4 Estimated ACS Weight/Power

Based upon the tentative selection of components indicated in the foregoing sections, the estimated weight and power requirements for the ACS are summarized in Table 6.4. As noted, the control electronics listed in this table include those needed for Auxiliary Propulsion System (APS). The rest of the hardware and propellant weights for the APS are separately covered in Section 6.4, however.

Candidate Momentum Wheel Characteristics

(Bendix Type 1880026)

Item	Value
Spin Inertia (slug - ft^2)	0.0647
Nominal Momentum -1400 rpm (ft-lbs-sec)	9 5
Stall Torque (oz-in)	20
Stall Power (watts, both phases)	53
Overall dimensions (inches) - outer diameter	12.125
- height	4.75
Weight (lbs, not including external electronics)	19.5
Synchronous speed (rpm)	1430

Table 6-3

Estimated ACS Weight and Power

Item		Weight (lb) Ea.	Weight (lb) Total	Power (watts) Ea.	Power (watts) Total	
Attitude Determination						
Earth Sensor (including electronics) (2)		4	8	5	10	
Sun Sensors and electronics (2)		1.5	3	1	2	
	Subtotal		11		12	
Momentum Wheel						
Wheel	(1)	19.5	19.5	--	--	
Wheel Electronics	(1)	10.5	10.5	53	53	max.
				20	20	avg.
	Subtotal		30		53	max.
					20	avg.
Control Electronics (ACS/APS)	(1)	6	6	20	20	max.
				10	10	avg.
	Subtotal		6		20	max.
					10	avg.
Passive Damper	(1)	2.9	2.9		-	
	Total		49.9		85	max.
					42	avg.

Table 6-4

6.4 AUXILIARY PROPULSION SYSTEM (APS)

The auxiliary propulsion system (APS) must provide the thrusters and total impulse needed for attitude control in the spin, acquisition, operational and backup operational (slow spin) control modes. In addition, it must fulfill the requirements for synchronous orbit correction maneuvers (300 ft/sec) in the spinning, operational and backup spin operational modes and for subsequent East-West station keeping and station relocation maneuvers (60 ft/sec) in the operational and backup operational modes. Thrust levels in the 0.5 to 1 pound range for spin precession control and in the 1-5 pound range for orbit control are needed.

The APS is to meet the indicated propulsion requirements for a mission duration time of up to 5 years. A major consideration in the definition of a preferred APS is the use of flight proven hardware wherever possible, and the use of redundancy for all critical elements to further enhance mission reliability.

6.4.1 Selection of a Preferred APS

Several propellants were considered for the reaction jets with particular attention to ammonia and hydrazine. The required, relatively high thrust levels and large impulse values, together with the advanced state of thruster and feed system development and considerable amount of flight experience, made hydrazine the preferred choice.

A number of companies, including Hamilton Standard Division of United Aircraft, TRW/Systems, Rocket Research Corporation and Marquardt, for

some time have been developing, testing and refining hydrazine feed system components and thrusters covering a wide thrust range. A variety of systems has been qualified, placed in production, and is in operational use on ATS, Intelsat and Air Force satellites.

Recent development has concentrated on the 0.1 lb. thrust level and on systems delivering millipound thrust levels. Catalytic thrusters at 0.5 lbF and above can be tailored for steady state or pulsed operation and are available in production models that have been qualified and flight proven. Table 6-5 is a summary concerning some of these candidate hydrazine thrusters.

The NETCOS is spin-stabilized during its coast period in the transfer orbit and during its synchronous orbit injection and initial correction maneuvers. Following this, the vehicle is despun, its solar panels are deployed, and it is inertially stabilized using a momentum wheel and jet torquers (3-axis) Attitude control thrusters at the 0.5 lb thrust level are needed to provide an adequate precession rate capability while spinning. Higher thrust levels are not needed because the satellite has been designed with a maximum moment of inertia about its stowed spin axis, thus making it inherently spin stable. This same thrust level can be used during the deployed operational mode because of the inherent gyroscopic stability provided by the momentum wheel running at a high bias speed.

Redundancy trade-off studies are discussed in the following section as regards a preferred configuration of the 0.5 lbF thrusters to meet all attitude control requirements. Also, as will be further discussed therein, orbit control requirements while spinning can be fully satisfied by symmetric firing of a central pair of the 0.5 lbF thrusters aligned with the spin axis. Alternatively,

Catalytic Hydrazine Thrusters

Thrust lb F	Hamilton Standard	Rocket Research	TRW
5	ATS-III Flight Tested Intelsat IV Similar to III Development problems with hard seat torque motor valves.	MR 50A Lockheed P-95 Satellite, 4 thrusters per module. All mode operation - Blowdown pressurization. Second order of 120 units, 4 units to AVCO proposed for Mars Lander (Viking 1973)	Intelsat III system. Blowdown @ 5↘1.2 lb F 90% steady state, 10% pulse (.080 on/.520 off) 2 redundant systems (2 tanks, 2 thrusters each)
1	Development Thrusters	MR 50A and MR 6A operated in the 1 lb-F range	Development thruster used for effect of environments on catalysts. (1967 Monopropellant Symposium)
0.5	Development Thruster	MR 6A thruster (classified HPM) 6 thruster, steady state operation, repressurization blowdown mode; supplying fourth system. Proposed for GE ERTS	Suggested for FHC ATS F&G, All mode operation with plenum or NH_3 for low thrust. (Proposed all ammonia system determined to be optimum)
.0.1	Proposed for GE ATS-F&G Extensive valve-thruster test. Pulse mode (.075 and .100 sec) and life testing	MR74 All mode development thruster. Proposed to GE for ATS F&G. Units to be delivered to JPL.	Development Thrusters
Notes	Extensive analytical effort at UA Research Labs on catalytic bed processes Data on Mid Range Thrusters, 5, 25, 15, 150, 200 lb-F	.05 lb-F Early development Proposed for Grand Tour mission Integrated plenum system delivered to GSFC	Plenum systems being flown on AF satellites

Table 6-5

appropriate pulsing of outward firing jets on the ±x sides (near the plane of the spacecraft CG) can be used for orbit control in this mode. Orbit control following deployment will be effected by use of the latter jets, activated by ground command at the appropriate position in orbit.

For those jet configurations where a central jet(s) aimed through the CG is considered for deployed orbit control, the 5.0 lbF thrust level is favored for fast, efficient orbit correction maneuvers.

6.4.2 Thruster Configurations

Various configurations of jets (location and number) were studied in arriving at a preferred configuration that would meet all thruster requirements with full backup redundancy for any failed thrusters. The proposed 12-jet layout seen in Figures 6-2 and 6-18 was arrived at through the logic next discussed.

The four-thruster diagram (Figure 6-18) represents a minimal, non-redundant configuration. There is no redundancy in translational thrust along the spin axis while spinning, in spin/despin (with unbalanced forces) around the spin axis, nor in in-orbit translational thrust. Translational maneuvers can only be done at one position in orbit. Since there is no torque around the x-axis, precession of the momentum wheel spin axis (y) in any inertial direction is accomplished by combining y axis maneuvers with z axis torquing. Such maneuvers would mean moving the panels off the sun line, possibly causing the antenna to lose the earth.

It is seen that the 4, 8 and 12a configurations do not have a thruster dedicated solely to in-orbit translational maneuvers. These are accomplished by an appropriate pair of parallel spin/despin jets, with a pulsed

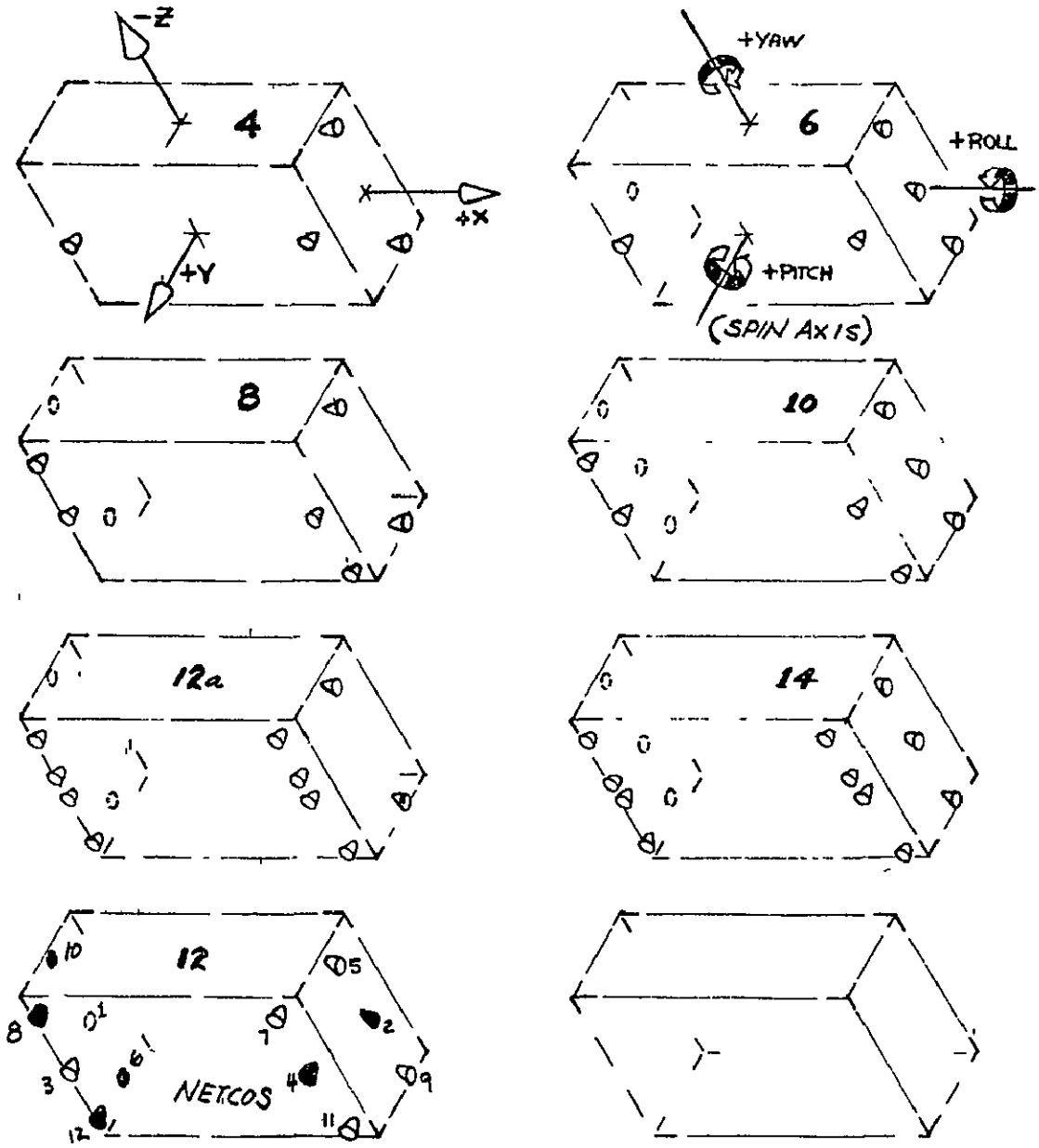

FIG 6-18 ALTERNATE JET CONFIGURATIONS

attitude control duty cycle in case of a thrust inbalance. With four jets there is no backup. With eight or twelve jets (as in 8 and 12a) failure of one spin jet would mean that orbital corrections could be made only once per orbit.

The eight-thruster configuration provides redundant translation thrusters along the spin axis in the spin mode, spin/despin couples around the spin axis with redundant single-thruster operation, an inefficient non-redundant torque around the x axis, and a redundant and coupled torque around the z axis. Failure of the x axis torquer would require going back to y axis maneuvers as a backup to provide momentum wheel spin axis precession in any direction.

The 12a thruster configuration provides full redundancy for the jets on the bottom of the module. Instead of placing the four additional jets side by side with those on the eight jet diagram, they are, as shown, placed opposite. This has the advantage of providing not only redundancy, but an efficient torque around x. The backup mode for x axis torque is then the same as the normal mode for eight jets, meaning that there is no need for y axis maneuvers which move the panels off the sun and disturb the earth-tracking antenna. Another advantage of this configuration over the previous one is that the redundant jets for translational thrust along the spin axis while in the stowed mode are located midway between the stowed panels therefore reducing the contamination danger to the panels

The right column of configurations shows what results when two opposing translational jets are added. If one of the two fails, its function can be taken over by the spin jets. In this case, the translation jets could be chosen with a greater thrust, i.e., 5 lbs, with all other jets at .5 lbs each.

Another option would be to add only one translational thruster and utilize symmetric thrusting of the spin control jets for backup translational maneuvers.

The twelve jet configuration, shown lower left, was chosen as the best compromise between simplicity and redundancy. The thrusters are grouped on two isolatable manifolds (odd numbers/open symbols/System A and even numbers/black symbols/System B) to compensate for valve open or catalyst bed failures. Prime and backup jet utilization for this configuration is summarized in Figure 6-19 for the NETCOS orbital configuration. During the transfer orbit when the stowed satellite is spinning, the two central +y firing jets are used for precession and orbit control.

6.4.3 Impulse Requirements and Propellant Load

The APS design to provide three axis attitude control and orbit control for the NETCOS has been sized to fulfill the following specific requirements:

- Despin from initial 90 rpm of Delta 3rd stage to 45 rpm
- 127-degree yaw precession to apogee injection orientation
- Precession control during transfer orbit coast
- Initial synchronous orbit correction, consisting of a 360-degree spin axis precession and a velocity impulse (ΔV) of 300 ft/sec
- Despin from 45 rpm to 0 rpm and acquisition of reference orientation
- East-West station keeping and station repositioning, consisting of a ΔV of 35 ft/sec (7 ft/sec/yr x 5 yr) for station keeping and a ΔV of 25 ft/sec for repositioning

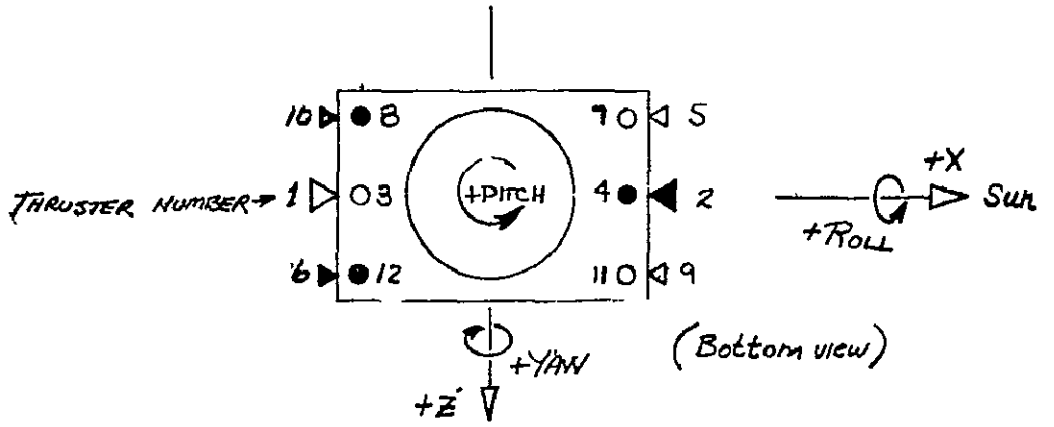

— ORBITAL CONFIGURATION —

	ROLL +	ROLL −	PITCH +	PITCH −	YAW +	YAW −	TRANS-LATION
PRIMARY (All Jets)	11 & 12	7 & 8	5 & 6 (COUPLED TORQUE)	9 & 10	3	4	1 OR 2
BACKUP (Sys A fail)	12 & [4] (CROSS COUPLING IN YAW)	8 & [4]	6	10	8 & 12	4	6 & 10 OR 2
BACKUP (Sys B fail)	11 & [3] (CROSS COUPLING IN YAW)	7 & [3]	5	9	3	7 & 11	1 OR 5 & 9

- ODD # Thrusters = Sys A; EVEN # = Sys B

NOTES:
- Thrusters #1 & 2 = 5 lbF, #3, 4, 5, 6, 7, 8, 9, 10, 11 & 12 = 0.5 lbF
- Thruster torquing uncoupled except for primary pitch
- The YY axis (PITCH) is the transfer orbit spin axis.
- Thrusters 3 & 4, 7 & 12 OR 8 & 11 used for spinning orbit control

FIG 6-19 NETCOS - 12 JET UTILIZATION

- Stabilization for 5 years against the dominant solar pressure torque
- Spin up to 1 rpm for wheel failure backup mode
- 50 percent attitude control contingency

Propellant calculations were made using current values for spacecraft inertias and mass and thruster moment arms, and specific impulses of 200 seconds and 230 seconds for pulsed and sustained thruster operations, respectively. These calculations indicated a total propellant load of 51.4 pounds, with 20 pounds for attitude control and 31.4 pounds for orbit control. As noted a 50 percent contingency was included for attitude control. No such reserve was added for orbit control because of the very conservative velocity impulse value used (300 ft/sec) for synchronous orbit correction maneuvers.

6.4.4 APS Configuration/Layout

Figure 6-20 illustrates the location of the jets and propellant tanks in relation to the apogee motor within the equipment module. Redundancy considerations and the design goal of maximizing the spin axis moment of inertia dictated a multitank arrangement close to the center of gravity.

The four hydrazine tanks, equally spaced around the apogee motor, are connected in opposite pairs to two thruster manifolds (systems A and B) while crossover lines equalize ullage pressures for tank pairs. Latching isolation valves and an interconnect line are configured to allow either or both tank sets to feed either or both thruster manifolds. This allows freedom in isolating thruster and thruster valve open failures as well as preventing total propellant loss. Latching isolation valves allow periodic use of particular

METCOS - .2 JET, 4 TANK SCHEMATIC LAYOUT

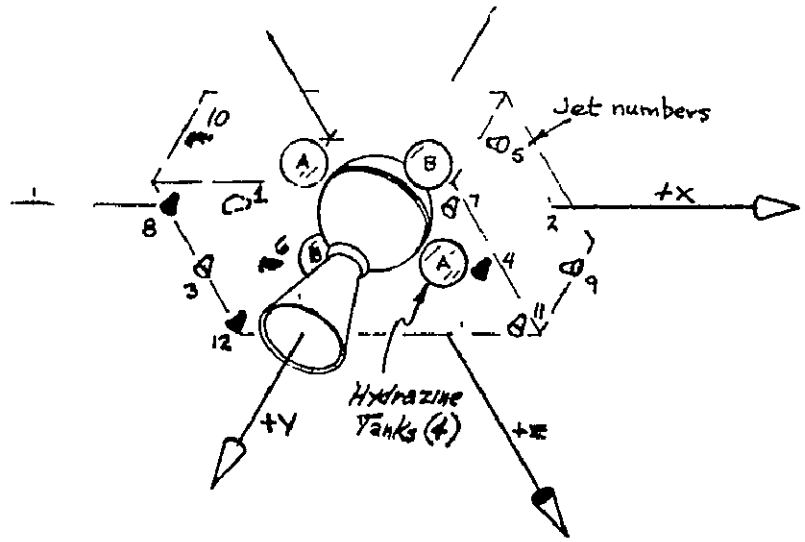

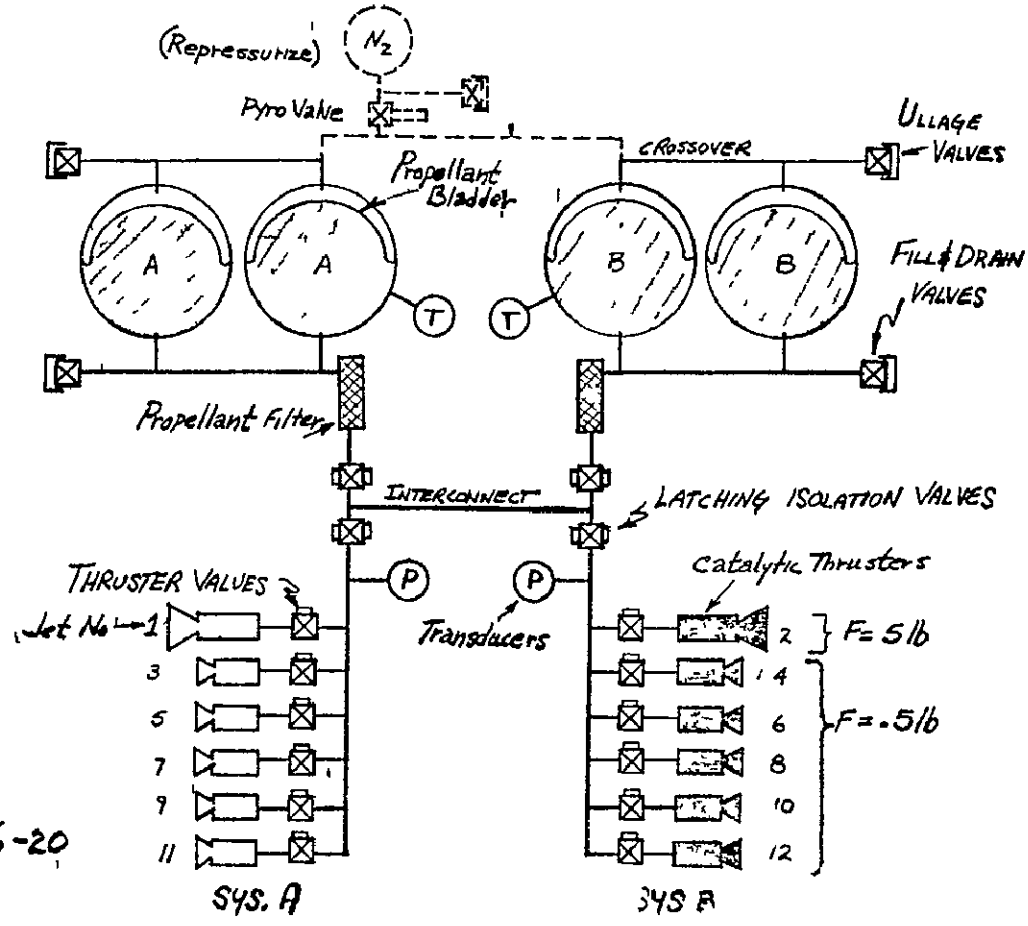

FIG 6-20

thrusters in either System A or B where other partially failed or degraded components exist, as well as use of residual propellant in isolated tanks. Systems A and B each provide a 3 axis torqueing capability and a translation or orbit control capability.

Tank volumes were determined using propellant density at 70°F. A 33% ullage volume was added to allow blow down operation of the feed system. Detailed studies of thruster operation and performance at final tank pressure will be necessary to determine the optimum ullage volume and initial pressurization level. It may be desirable to include a small high pressure nitrogen bottle to repressurize the system to its initial level after partial propellant usage or as backup pressurization.

While solenoid valves remain a potential problem, concerted efforts in recent years by hydrazine system suppliers, in the areas of contamination control, materials selection, and mechanical design have resulted in a number of proven dependable designs. Further, the APS system has been designed with considerable flexibility and redundancy, both in propellant feed and in jet utilization, so as to ameliorate the effects of any valve failures.

The estimated weight for the APS is itemized in Table 6-6. It totals 72.7 pounds.

Table 6-6

Auxiliary Propulsion System Weight

Item	Quantity	Weight (each (lbs)	Weight (total) (lbs)
Propellant Tanks	4 (11.5" dia)	2.3	9.2
Propellant			
Attitude Control			17.1
Orbit Control			31.3
Pressurant			1.0
Fill and Drain Valve	2	.28	.6
Pressure Transducers	2	.32	.6
Isolation Valve	4	.63	2.5
Thermocouple	2	.06	.1
Filter	2	.40	.8
Fitting and Lines		2.51	2.5
0.5 # F Thruster and Valve Assembly	10	.55	5.5
5.0 # F Thruster and Valve Assembly	2	.75	1.5
			72.7

APPENDIX A

Representative NETCOS Solar Torque Calculation

(Rotating Feed - Parabolic Reflector)

The predominant attitude disturbance effect on the NATS results from solar pressure. The large solar panel area and the long antenna arm create torques on the order of 10^{-4} in. lb. which must be made to balance each other. There are also smaller torques acting on the body of the spacecraft.

The basic equations used to calculate solar force components as shown in the diagram are

$$F_n = \left[\frac{2}{3}\rho\ (1 - s)\cos\Psi + (1 + s\rho)\cos^2\Psi\right] KA\bar{n} \qquad \text{(normal)}$$

$$F_t = (1 - s\rho)\ KA\cos\Psi\sin\Psi\ \bar{t} \qquad \text{(tangential)}$$

where,

ρ = reflectance

s = 0 for totally diffuse reflectance

1 for totally specular reflectance

K = solar force constant, 10^{-7} lb/ft^2

A = Total Surface Area, ft^2

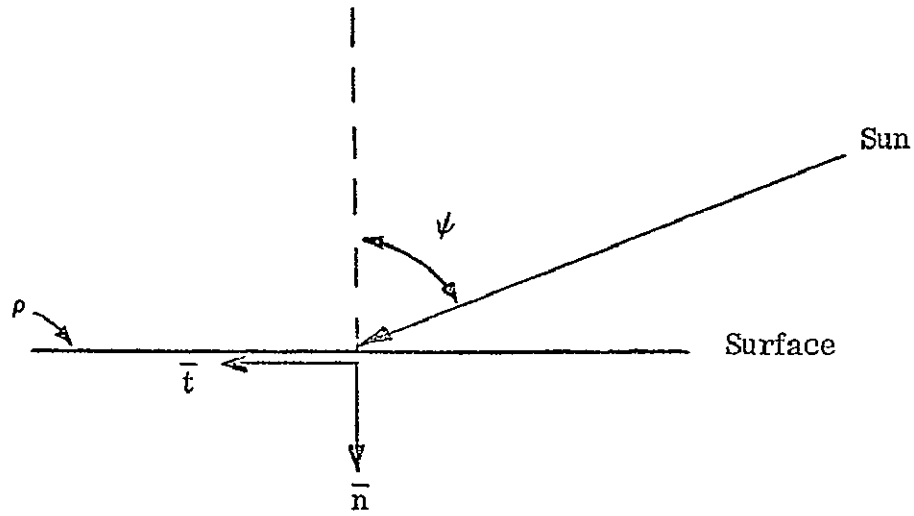

Diffuse reflectance was assumed on all surfaces except those of the top (rotating) box (see Figure 1). To find the force on the antenna, the dish was approximated as a portion of a sphere, and the given force equations were integrated over its surface. The results, for full view and side view of the antenna are:

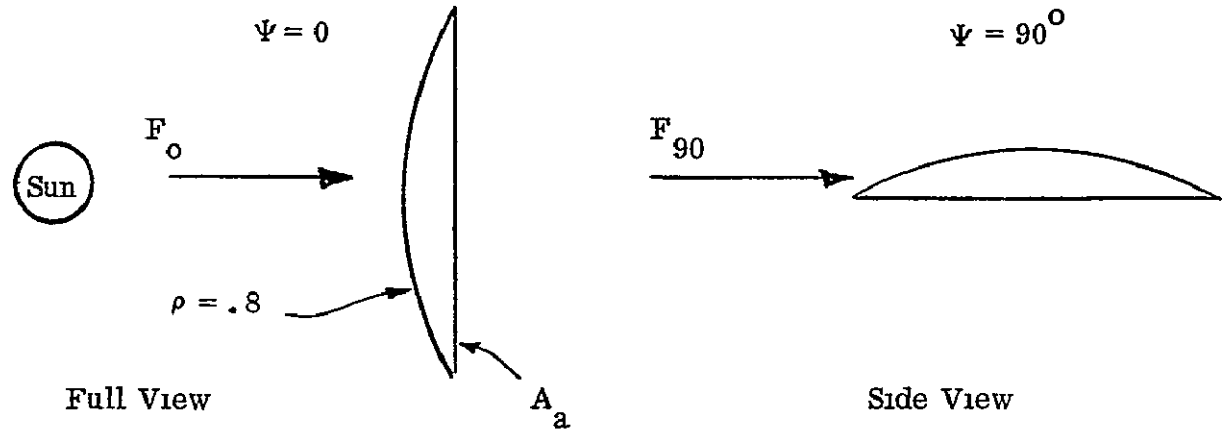

$F_o = 1.46\ K\ A_a$ lbs

$F_{90} = .134\ K\ A_a$ lbs

A_a = full view projected area = 12.56 ft^2

Using these formulas and the constants of Table 1, the force on each surface is calculated, and when multiplied by its moment arm gives the contribution to solar torque of that surface. The results, for equinox and solstice conditions, are presented in Table 2. Tangential force on the panel has no moment arm (since the CG lies in the plane of the panels), and therefore is not listed. It should be noted that during solstice the angle between the sun line and the normal to the box sides is $\Psi = \cos^{-1}(\cos(45)\cos(23.5))$ The only force which has not been calculated is that on the rocket nozzle.

It is assumed that at equinox the total $\pm$ moments will be balanced. Thus, taking all other distances from the center of gravity as fixed, the position of the center of the panels, r_p, is found which, at equinox, gives an average moment of zero between the two extreme antenna views (full and side). The moment arms and their magnitudes are shown in Figure 1. Once r_p is set, the total moment for each orbital position of interest is calculated. The results appear in Table 3.

Assuming that attitude correction is performed at the terminator plane (antenna, side view), the maximum precession due to the periodically varying solar torque (2 cycles per orbit) during half an orbit occurs about three/nine hours later. Using the equinox condition maximum moments and the formula for angular precession.

Table 1. Component Areas/Reflectances

			Top Box		Bottom Box	
Surface	Panels	Antenna	Top	Sides	Bottom	Sides
Area, ft.^{2}	99.46	12.56	18.8	5.56	18.8	9.72
Reflectance (s=0)	.2	.8	.92 (s=1)	.92 (s=1)	.5	.5

Table 2. Component Torques

		Antenna		Top Box		Bottom Box	
Surface / Moment x 10^7, in. lb.	Panel	Full	Side	Top	Sides	Bottom	Sides
Equinox	$-112.7\ r_p$	$18.34\ r_a$	$1.68\ r_a$	0	$3.93\ r_{xt}$	0	$8.5\ r_{xB}$
Solstice Winter	$-95.8\ r_p$	$16.82\ r_a$	$1.54\ r_a$	0	$3.304\ r_{xt} \pm 4.06$	$-6.8\ r_B$	$-7.27\ r_{xB} \pm 44.45$
Solstice Summer				$.55\ r_t$		0	

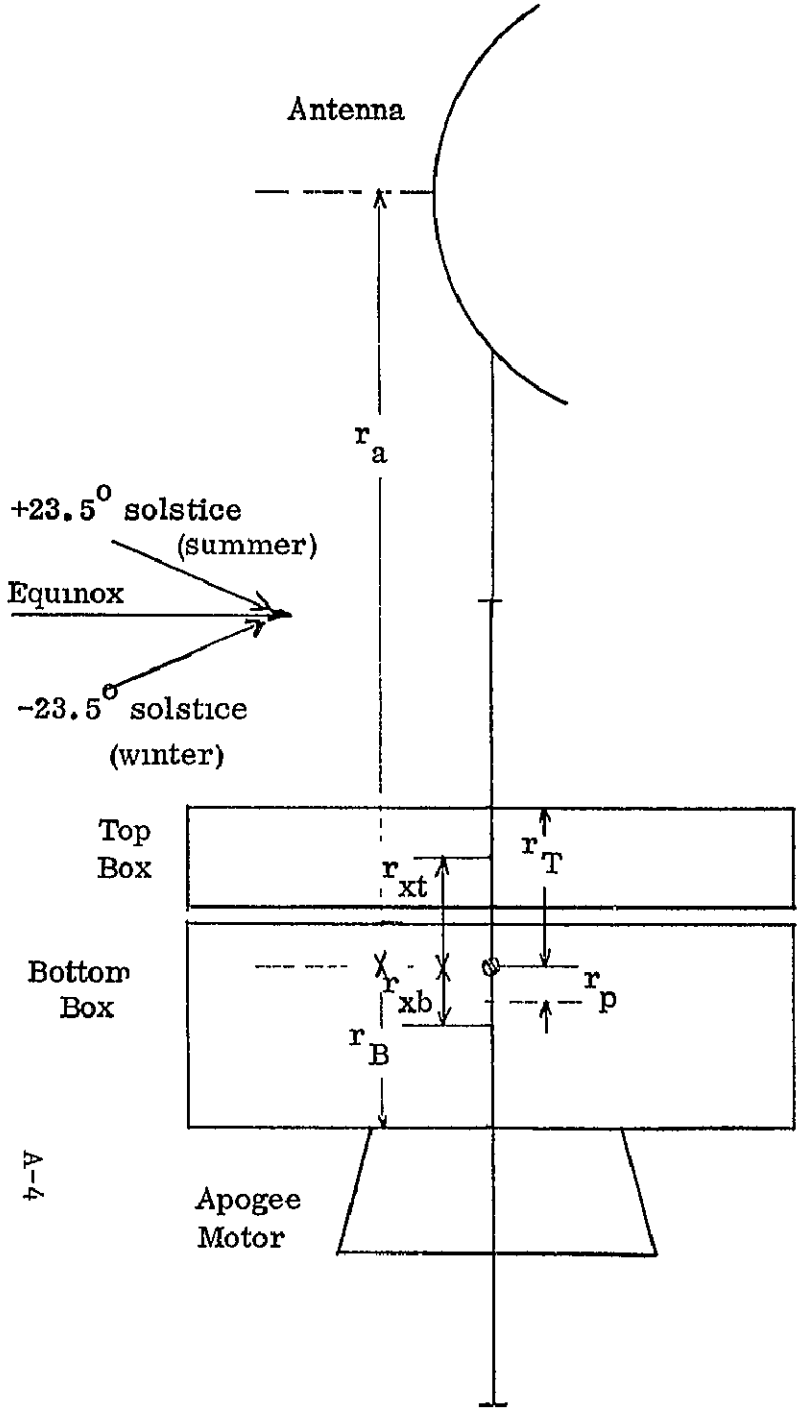

r_a = 56.6 in

r_{xt} = 9.1

r_{xb} = 5.9

r_t = 13.1

r_b = 12.9

r_c = 25

r_p = 4.9

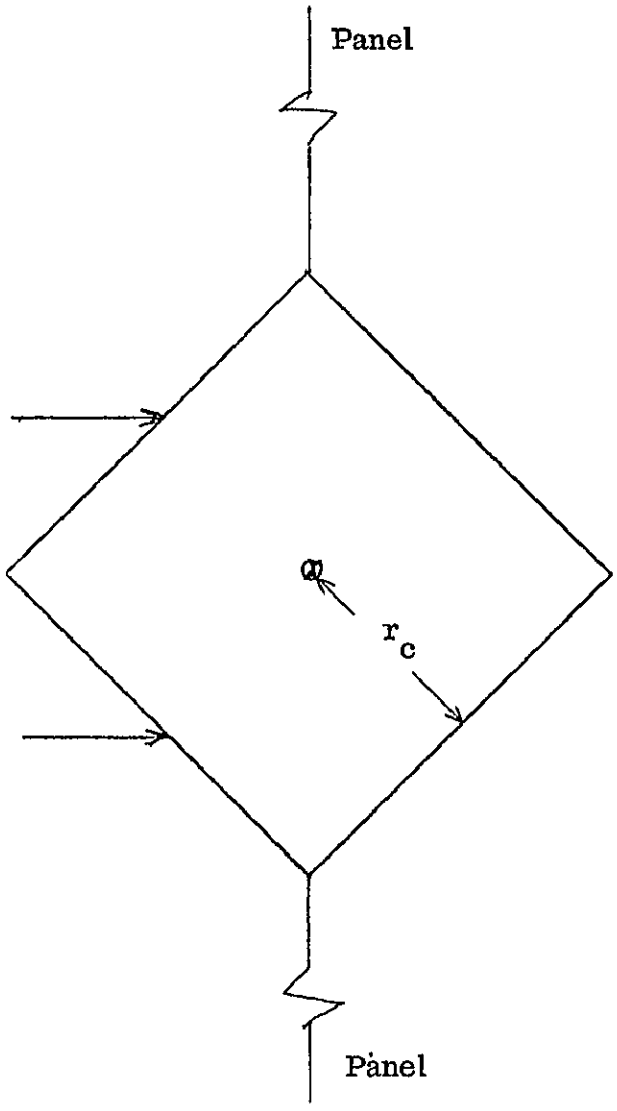

Figure 1.

Table 3. Total Solar Torque

Orbital Condition / Antenna Position	Equinox	Solstice	
		+23.5 degrees	-23.5 degrees
0^{o}	$+472 \times 10^{-7}$ in. lb.	$+423 \times 10^{-7}$	$+431.x\ 10^{-7}$
90^{o}	-472×10^{-7}	-436×10^{-7}	-434×10^{-7}

$$\theta = \frac{Mt}{H}$$

where:

M = torque t = time

H = angular momentum of inertia wheel = 9.5 ft. lb. sec,

the maximum precession for the half-orbit is found to be 0.18 deg. This is within the prescribed control limit of 0.5 deg. It is reiterated that it is planned to balance the average of the varying antenna torque with the solar panel torque. Hence, the indicated precession angle will reverse in direction with each quarter orbit.

While the bias value of solar torque is nominally zero at equinox, it will be -3 and -1.2×10^{-7} in. lb., respectively, for the summer and winter solstice conditions. Taking the average bias torque for five years, the propellant weight required to counter the secular precession is,

$$W_p = \frac{Mt}{I_{sp}\, r}$$

I_{sp} = 230 sec.

r = jet moment arm = 25 in.

$\therefore W_p = .003$ lb.

Secular precession also occurs if there is an error in the planned CG and/or CP positions. Assuming a half-inch offset, its effect for each condition is found by multiplying the sum of the solar forces by a half-inch moment arm. These offset moments are in addition to the ones in Table 3. For the equinox, full antenna view condition, the additional moment is 72×10^{-7} in. lb. The average for all six orbital conditions is 73×10^{-7} in. lb., which when acting for five years requires 0.20 lb. of propellant to correct. This figure includes the panel tangential force acting on a half-inch arm; it must be doubled to cover offsets in two orthogonal directions relative to the sun line.

The precession angle for a full orbit due to an offset along the North/South (antenna) axis is .35 deg. during winter solstice. Hence correction of this angle build-up would only be required once a day. This angle plus the oscillating precession angle would then be $\leq .5$ deg. If each correction is programmed to overcorrect the precession by .35 deg., the frequency of correction can be reduced to once every other day.

Conclusions

Proper positioning of the CG and solar panels relative to the antenna can balance solar torques well enough that precession during an orbit will stay below the required limit, and will reverse in direction four times per orbit. By properly biasing the precession corrections, a correction need be made only every other day. The long term effect of countering solar torque, with a half-inch error in CP-CG location, will involve only 0.2 lbs. of propellant for each of two control axes. The torque about the Y axis, perpendicular to the orbital plane, is small enough to be countered by the wheel, and has no secular term.

APPENDIX B

REVISED WEIGHT TABLES

During the month of July 1970 additional analyses and investigations were performed in order to refine some of the assumptions contained within this report. Coincidentally additional information became available which increased the Delta launch vehicle capability by approximately 55 pounds. The following weight summary tables reflect the increased launch capability as well as a refinement of the various system and component weight.

Table B-1 Spacecraft Weight Summary

Item	Weight (lbs)
Power System	186.0
Communications System	59.7
TM and Command System	26.3
Antenna System	9.2
Attitude Control System	49.9
Auxiliary Propulsion System	74.9
Thermal Control System	15.0
Electrical Distribution System	30.0
Structural System	89.7
Apogee Motor Inerts (burn-out)	46.4
Weight Growth	100.4
Total Payload	687.5
Apogee Motor Propellant	614.5
Separation Weight	1302.0
Adapter (launch vehicle)	53.0
Gross Weight	1355.0

Table B-2 Power System Weight Summary

Item	Weight (lbs)
Battery (2)	51.8
Battery Charge Regulator (1)	3.0
Battery Discharge Regulator (2)	8.0
Voltage Limiter (2)	8.0
Power Control Unit (1)	11.0
Solar Array (including deployment system)	104.2
Total Weight	186.0

Table B-3 Telemetry and Command Weight Summary

Item	Weight (lbs)
Command Receivers (2)	2.6
Command Decoder (2)	8.0
Command Regulator (2)	1.0
TM Multiplexer (2)	8.0
TM Switching Unit (1)	1.0
TM Transmitters (2)	0.8
Diplexers (2)	2.0
T & C Antenna Hybrid (1)	1.9
T & C Antenna Elements (4)	1.0
Total Weight	26.3

Table B-4 Communication System Weight Summary

Item		Weight (lbs)
L Band		
Diplexer	1.7	
Pre-amplifier	0.5	
Down-Converter	1.8	
Up-Converter (5)	2.1	
PA Driver & Hybrid (5)	1.6	
Power Amplifier (5)	20.8	
		28.5
C Band		
Diplexer	1.0	
Pre-amplifier (2)	0.5	
Down Converter	1.4	
Up Converter (2)	1.8	
Power Amplifier (2)	0.5	
		5.2
IF Amplifier		3.5
Synthesizer		6.0
Switches		1.5
IF Switching Matrix		1.0
MDA and Electronics		
Motor-fixed feed		8.0
Drive Electronics		6.0
	Total Weight	59.7

Table B-5 Attitude Control System Weight Summary

Item	Weight (lbs)
Electronics	6.0
Inertia Wheel	30.0
Attitude Determination	11.0
Passive Damper	2.9
Total Weight	49.9

Table B-6 Auxiliary Propulsion System Weight

Item	Weight (lbs)
Propellant Tanks (4) (11.5" dia)	9.2
Propellant	
Attitude Control	18.0
Orbit Control	32.6
Pressurant	1.0
Fill and Drain Valve (2)	0.6
Pressure Transducers (2)	0.6
Isolation Valve (4)	2.5
Thermocouple (2)	0.1
Filter (2)	0.8
Fitting and Lines	2.5
0.5 #F Thruster and Valve Assembly (10)	5.5
5.0 #F Thruster and Valve Assembly (2)	1.5
Total Weight	74.9

Table B-7 Structural System Weight Summary

Item	Weight (lbs)
Lower Frustum	8.3
Module Support Ring-Lower	1.9
Apogee Motor Ring	3.7
Module Support Ring-Upper	1.2
Cylinder (stiffened)	11.9
Module Structure (including solar array support structure)	55.4
Upper Frustum	1.7
Bearing, Inner and Outer Ring	2.3
Separation Ring	3.3
Total Weight	89.7

Table B-8 Miscellaneous Weight Breakdowns

The following three tables are detailed breakdowns of items presented in previous tables and are not additive with previous tables.

Item	Weight (lbs)
Module Structure Weight Summary (see Table B-7)	
Sides	20.9
Top and Bottom Skins	9.8
Bulkhead Webs	3.9
Bulkhead Framing Members	2.5
Edging Members	6.3
Miscellaneous	6.0
Solar Array Retention Mechanism	6.0
Total Weight	55.4
Solar Array Weight Summary (see Table B-2)	
Deployment System	2.0
Cell Stack	36.3
Thermal Paint	6.9
Structure	
Faces	17.3
Glueline	13.8
Core	18.7
Edging Members	6.0
Fittings (Attachment Sect.)	2.0
Hinges	1.2
Total Weight	104.2

Table B-8 Miscellaneous Weight Breakdowns (Cont'd)

Item	Weight (lbs)
Module Equipment Weight Summary	
Attitude Control	49.9
Auxiliary Propulsion	15.1
Power (less array)	81.8
Communication	59.7
Thermal	15.0
Electrical Distribution	30.0
Telemetry and Command	26.3
Total Weight	277.8